MASTER THESIS

Vascularized bone marrow model for studying a breast tumour to bone metastasis using a multi-organ-on-a-chip approach.

S.T. Stevers

Applied Microfluidics for BioEngineering Research (AMBER)
Faculty of Science and Technology (TNW)
Faculty of Electrical Engineering, Mathematics and Computer Science (EEMCS)
University of Twente

Examination Committee:
dr. ing. A. Zuchowska (Daily Supervisor)
prof. dr. ir. S. Le Gac (Committee Chair)
prof. dr. A. Koçer (External Member)

<DATE>

UNIVERSITY OF TWENTE.

ACKNOWLEDGEMENT

I would like to thank my supervisors for their continuous support during my research project. Firstly, I would like to thank my daily supervisor Agnieszka Zuchowska. Thank you for all the help in the lab and for the feedback on my report as well as making the beautiful confocal images for me. Also, good luck with your new position in Poland.
Secondly, Séverine le Gac for all the feedback on my report and presentations during the project as well as for the discussions about the experimental approaches.
Furthermore I would like to thank Armagan Koçer for taking place in my graduation committee, your interest in the project, and making time to review my work.
Also, thanks to Carlo Alberto Paggi and Tomas van Dorp for helping me with the design and implementation of the qPCR experiments as well as the discussions about the experiments.
Finally, I would like to thank all the DBE and AMBER members and students for the support during my project. Especially for the well appreciated coffee breaks and fun times on and off the lab.

ABSTRACT

Cancer has a growing incidence worldwide and metastases represent the primary cause of death from cancer. However, there is still a lot unknown about the mechanisms that support metastasis to specific organs. Bone marrow is one of the most frequently metastasized sites for different types of cancer such as, beast and prostate cancer. Therefore, a lot of research is performed into the understanding, prevention and treatment of the metastasis. To this end, in this work, a bone-marrow-on-chip is developed that can be connected with a vascular circulation to a tumour tissue.

The development of a representative bone marrow tissue on chip is presented to actually be used for mimicking metastasis to bone marrow. First the hydrogel is investigated to form a bone vascularized tissue. To do so, the amount of self organization and migration of cells cultured as spheroids in the hydrogels is analyzed. Both Collagen I and Fibrin hydrogel are used, and from these two Fibrin hydrogel showed the best potential for vascularization of the spheroids.

Next, the spheroid composition is structured considering bone marrow derived mesenchymal stem cells (MSCs), osteoblasts (OBs) and endothelial cells (ECs) of two types. First, the spheroids are formed in round bottom microwells and after two days injected into the hydrogel. Now the spheroids are cultured for 7 days in well plates during and after which various analysis methods are used to analyze the effect of different conditions. These analyses include quantification of the migration of cells in the hydrogel, immunostaining and quantitative polymerase chain reaction (qPCR). MSCs are combined with HUVECs to improve the vascularization of the tissue and with OBs to form a more representative bone marrow. Also, the effect of bone marrow endothelial cells (BMECs) on both MSCs and OBs is investigated to see the effect of the tissue specific ECs. In the end a triple culture of MSCs, OBs and BMECs was identified as the best cellular composition for the vascularized bone marrow formation.

After the experiments with spheroids in wells plates, the best conditions are selected to be performed on chip. The on chip cultures however did not show the same results as the wells plate cultures. As of now there is no clear reason why but this has to be investigated further. Also, the qPCR has to be performed again to obtain more data points and control measurements from the different conditions.

SAMENVATTING

Kanker is een groeiend probleem wereldwijd en metastases naar andere organen is een van de meest voorkomende doodsoorzaken die hierbij komen kijken. Er is op dit moment nog veel onduidelijk over de precieze mechanismes waardoor een kanker vaak naar een specifiek orgaan metastaseert. Er wordt veel onderzoek uitgevoerd om deze metastases beter te begrijpen, voorkomen en te behandelen. Een metastase naar het beenmerg komt bij verschillende type kanker erg vaak voor. Om de mechanismen die hiervoor zorgen beter te begrijpen, is beenmerg op een chip ontwikkeld die via een vasculaire circulatie aangesloten kan worden op een weefsel met een primaire tumor.
In dit verslag is gevasculariseerd beenmerg op chip ontwikkeld, die gebruikt kan worden om de metastase naar beenmerg na te bootsen. Eerst is een optimale hydrogel onderzocht voor het vormen van een gevascullariseerd weefsel. Hiervoor wordt de hoeveelheid zelforganisatie en migratie van cellen gekweekt als sferoïden in een hydrogel geanalyseerd. Een Collageen I en Fibrine hydrogel worden hiervoor gebruikt en hiervan bleek in Fibrine de beste vascularisatie van de sferoïden mogelijk.
Vervolgens wordt de optimale sferoïde samenstelling van beenmerg geïsoleerde mesenchymale stamcellen (MSCs), osteoblasten (OBs) en endotheelcellen (ECs) bepaald. De sferoïden worden in twee dagen gevormd in ronde bodem microwellen en vervolgens verplaatst naar een hydrogel. De sferoïden worden dan voor 7 dagen gecultiveerd in well platen waarna verscheidene analysemethoden uitgevoerd worden om het effect van verschillende condities te bepalen. Onder deze analyses vallen de kwantificatie van de cel migratie, immunokleuring en kwantitatieve polymerasekettingreactie (qPCR). Vervolgens worden MSCs gecombineerd met endotheelcellen van menselijke navelstrengaders (HUVECs) om de vascularisatie te verbeteren en met OBs om een beter representatief beenmerg weefsel te vormen. Vervolgens wordt er gekeken wat het effect is van het combineren van uit beenmerg geïsoleerde endotheelcellen (BMECs) met MSCs en OBs, om te kijken wat het effect is van het gebruiken van weefselspecifieke ECs. Uiteindelijk wordt een drievoudige cultuur geïdentificeerd als best conditie voor het maken van gevascullariseerd beenmerg weefsel.
Na de experimenten in well platen worden de beste condities geselecteerd voor de op chipculturen. De resultaten van deze op chipculturen zagen er echter anders uit dan de well plaat culturen. Hier is op dit moment nog geen duidelijke verklaring voor en dit moet dan ook verder onderzocht worden. De qPCR data die al is verzameld mist ook nog datapunten waardoor er nog geen volledige conclusie uit getrokken kan worden, deze zal nogmaals uitgevoerd moeten worden en een controle meting voor meerdere condities zal toegevoegd moeten worden

CONTENTS

ABBREVIATIONS

2D	Two-dimensional
3D	Three-dimensional
AsAP	Ascorbic acid 2 phosphate
BMECs	Bone marrow derived endothelial cells
CTCs	Circulating tumor cells
ECM	Extracellular matrix
ECs	Endothelial cells
EDTA	Ethylenediaminetetraacetic acid
EGM-2	Endothelial Cell Growth Medium-2
EthD-1	Ethidium homodimer-1
FBS	Fetal bovine serum
GAPDH	Glyceraldehyde 3-phosphate dehydrogenase
GFP	Green fluorescent protein
HA	Hydroxyapatite
HECF-ECs	Human endothelial colony forming cell-derived endothelial cells
HSCs	Hematopoietic stem cells
HUVECs	Human umbelical vein endothelial cells
MSCs	Mesenchymal stem cells
NHLFs	Normal human lung fibroblasts
OBs	Osteoblasts
OoC	Organ-on-chip
PBS	Phosphate-buffered saline
PDMS	Polydimethylsiloxane
pen/strep	Penicillin-Streptomycin
PFA	Paraformaldehyde
qPCR	Quantitative polymerase chain reaction
RFP	Red fluorescent protein
RNA	Ribonucleic acid
RT	Room temperature
TEM	Transendothelial migration
TRIS	Tris(hydroxymethyl)aminomethane
VFP	Viscous finger paterning

1 INTRODUCTION

1.1 Cancer

Cancer has a growing influence on the healthcare system worldwide, and its incidence continues growing as well as mortality associated with cancer and more than 19 million new cases and almost 10 million cancer related deaths worldwide in 2020 [1]. When a cancer is present, there is a high chance of metastasis to other organs, and some types of cancer have a higher risk of metastasis than others, like melanoma, breast and kidney cancer [2]. Furthermore, metastases account for 90% of cancer-related deaths [3]. Due to this high mortality there has been a focus on understanding and preventing metastasis [4]. Bone is one of the most frequently metastasized sites, and primary breast cancer in females and/or prostate cancer in males, account for the majority of the skeletal metastases [5]. Breast cancer will metastasise to bone in 55 % of all cases compared to the second most common metastatic site, the lungs, with a 30 % chance of metastasis [6]. Moreover, other types of bone metastasis, from lung and kidney for example, are also possible. Thus, bone models can be used to investigate a multitude of primary cancer metastasis to bone. Altogether, bone metastasis has a extremely poor prognosis and is accompanied by chronic pain, decreased mobility and other secondary symptoms, which all cause a significant decrease of quality of life of the patient. This is why there is a lot of research performed into the understanding, prevention and treatment of this type of metastasis.

1.1.1 Metastasis

For a primary tumour to cause a metastasis tumour cells have to go through a series of steps and overcome a number of obstacles. These obstacles include; the escape from their primary site by crossing the endothelial barrier into the bloodstream, harsh conditions in the bloodstream circulation, adherence to the vascular wall, crossing the endothelial barrier once more to entering the tissue, acclimating to the new microenvironment and escape from immune cells during all the processes [7]. As a direct consequence, fortunately the chance of forming a metastasis is very low [8], with only 0.001-0.02 % of all cancer cells that enter the circulation forming a metastasis [9]. However, when a metastasis has been established this is hard to detect and our treatments frequently fail to combat the secondary tumour [8]. There are correlations between the primary and secondary site of the cancer, like breast cancer tends to metastasize into multiple organs like bone, liver, brain and lungs, with the highest probability for bone marrow [10]. This preference can be partially explained by the permeable sinusoidal vessels that some tissues have, like in the bone tissue, which increases the rate of metastasis [11]. However, a lot of studies aim to explain the correlation between the tumour type and the targeted organ which is mostly explained by a seed that seeks a specific soil [12]. This ”seed and soil” hypotheses was fist described by Stephen Paget in 1889 [13]. The different steps of metastasizing are shown in Figure 1.1. The primary steps of a cancer metastasis are intravasation, circulation, extravasation and colonization; these four steps will be further elaborated below.

Intravasation

Intravasation is the invasion of tumour cells through the endothelial layer of the vasculature into the blood or lymphatic vessel [14]; this process is active or passive [15]. This mediation depends on the tumour type, TEM and vasculature [11]. 3D microfluidic models have shown that the endothelial lining is a barrier for the intravasation which is regulated by the TEM [16]. Due to these constraints the tumour cells have to squeeze themselves through a tight barriers which causes

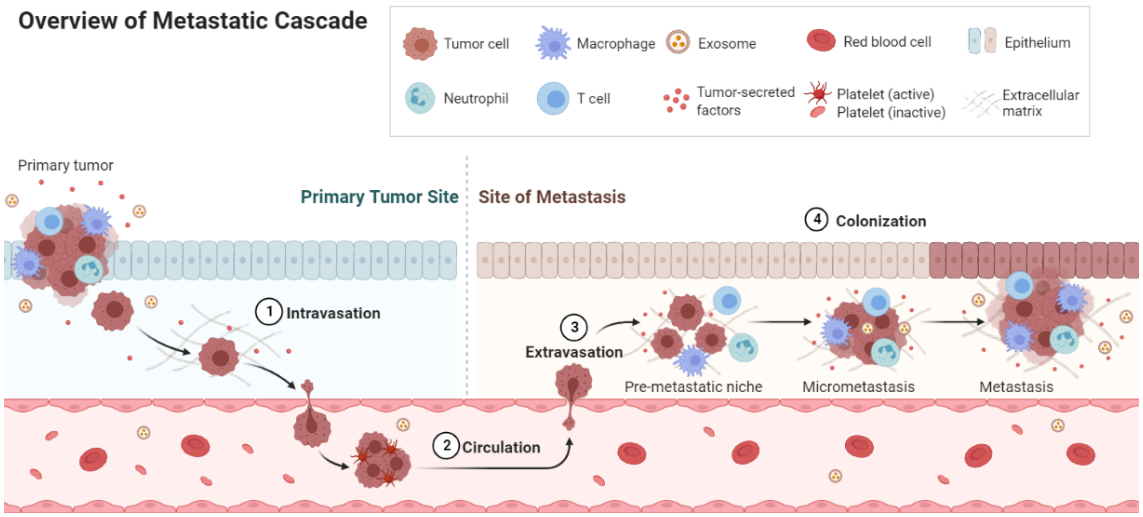

Figure 1.1: Schematic overview of the metastatic cascade. The four major steps intravasation, circulation, extravasation and colonization. Created with BioRender.com

the nuclear envelope to loose integrity, DNA damage and rearrangement, which in turn increases the metastatic potential of the cells when repaired [17]. It has also been shown that the epithelial-mesenchymal transition, which causes the epithelial cells to loose their adhesion potential and gain invasive properties, plays a important role in the tumour cells' ability to escape the tumour environment and enter the circulation [18, 19].

Circulation

When tumour cells have left their primary site and entered the blood or lymphatic system they are called CTCs until possible extravasation at a distant site. The interactions of the CTCs with the environment in the circulation determine their change of survival and extravasation [20]. CTCs can circulate as a single cell or clusters, formed by the presence of cell junction component plakoglobin will increase the metastatic potential [21]. The formed clusters comprise more than only CTCs, stromal cells and immune components from the primary microenvironment that enhance the survival chances [19, 21]. The clusters will also interact with blood platelets that allow the cluster to shield itself from the shear forces and escape immune detection [22, 23, 24]. When CTCs adhere or become trapped in small capillaries they, either extravasate into the tissue, or grow within the vessel before extravasation happens [7, 25].

Extravasation

Extravasation is performed by induced local vessel remodelling of the endothelial layer by the CTCs [25]. When CTCs adhere or become trapped in a capillary they undergo interactions between the microvascular endothelium that will allow for cytoskeletal changes that are required for the TEM [26] or it can lead to a microvascular rupture [8]. Extravasation is a complex process that relies on different ligand receptor interactions, chemokines and circulating non-tumour cells and is not yet fully understood due to the lack of models that are capable of the identifying the precise mechanisms [26, 27].

Colonization

When tumour cells have entered a secondary site they can go into a dormant state and remain quiescent or start proliferating which is called the colonization [11]. When a metastasis is formed supply of nutrients and oxygen is especially important; therefore tumour secrete angiogenic factors to recruit ECs, which will induces the vessel formation [28].

1.2 Bone marrow

Due to its higher endothelial permeability and the ”soil” function of the bone it is a important factor in the metastasis of cancer. Bones are composed of a cortex and medulla; the cortex is a layer of strong compact tissue and the medulla a porous structure, which houses the bone marrow in its interstices [29]. Bone marrow is home to the essential pluripotent precursor cells for the human body [30]. The primary functional cell types are the HSCs, which play a crucial role in the renewal of all types of blood cells [31]. Next to HSCs, the marrow contains MSCs, which are multipotent stromal cells that are capable of differentiation into types of cells, such as osteocytes, chondrocytes, and adipocytes [32].
The bone marrow can be divided into red and yellow marrow; the red marrow contains primarily hematopoietic and mesenchymal stem cells and the yellow marrow is largely composed of adipose tissue [29]. At birth, the marrow is entirely red marrow, however during aging red marrow contracts and be replaced by yellow marrow. In adults the red marrow is mainly located in the spongy bone in the epiphysis and the yellow marrow in the diaphysis. The structure of the bone and location of the different marrow (cell) types is illustrated in Figure 1.2. Since only the red marrow contains the HSCs, it can be considered as the functional part of the bone marrow. Because of the relatively higher microvascular density of the bone marrow it has been associated with an increased tumour metastasis incidence [33]; it is as well a favorable environment that can support tumour growth and survival [34]. From the different marrow types a metastasis is more likely to occur in the better vascularized red marrow [35].

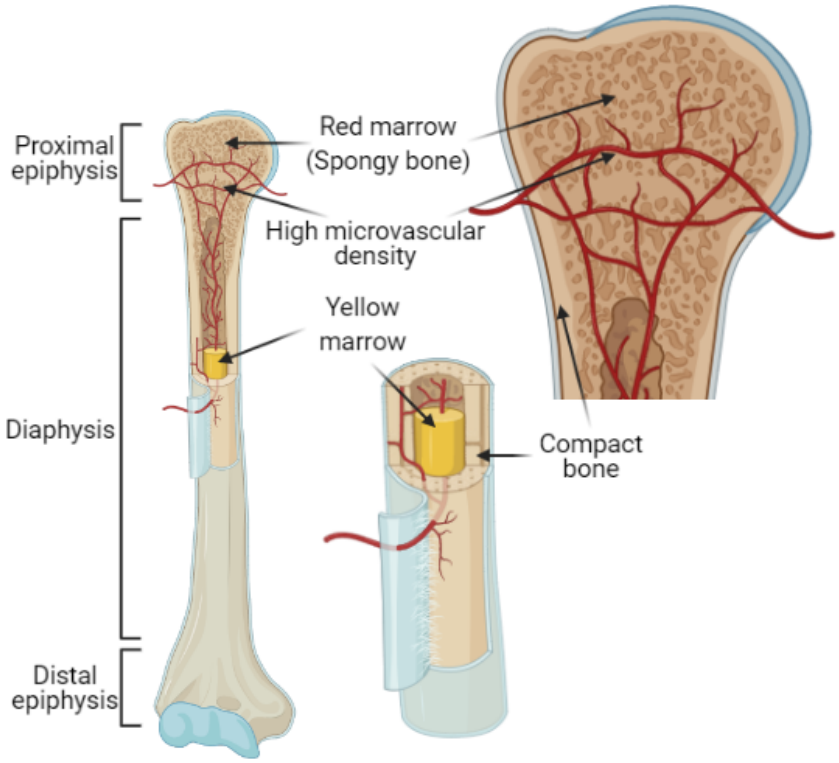

Figure 1.2: Schematic structure of the bone showing the location of the red and yellow bone marrow indicated as well as the higher microvescular density. Created with BioRender.com

Apart for the blood cell producing HSCs, the MSCs are the structural maintaining cells of the marrow, these cells maintain the microenvironment in which the HSCs are housed. The MSCs work in cooperation with a small number of osteogenic cells that have migrated into the marrow, two of these cell types being derived from the MSCs. There are three main osteogenic cells present in the bone; the osteoblasts, osteocytes and osteoclasts. OBs are bone-forming cells and have three main functions; production of bone matrix (osteoid), regulation of osteoid mineralization by production of non-collagenous proteins and supporting the osteoclast formation [36]. When OBs have completely surrounded themselves in mineralized ECM they further differentiate into osteocytes [37]. Osteocytes are cells that are present in their own lacunae, which they create by

surrounding themselves in mineralized matrix [38]. These cells have a monitoring function that can sense stress and strain in the bone; this information is next passed down to the osteoblasts and osteoclasts to induce bone remodelling [39]. Osteoclasts are cells derived from HSCs and have a role similar to macrophages; these cells reabsorb the bone matrix when activated [40]. The ECM that is produced by the MSCs consists of various proteins such as proteoglycans or glycosaminoglycans, fibronectin, tenascin, collagen, laminin, hemonectin, and thrombospondin [41].

1.3 State of the art bone models

1.3.1 Bone marrow *in vitro* models

Because the functional bone marrow comprises different cell types, models should include these different cells. So, to mimic the remodelling capacity of the bone HSCs and/or differentiated osteoclasts must be incorporated into the model. When only the formation of the bone structure is required, MSCs can be sufficient to form the ECM [42]. There have been different approaches to fabricate representative 3D structures of tissues including the bone which are combined with the required cell types; spheroids, scaffolds and hydrogels [43].
Spheroids are 3D spherical clusters of cells of one or multiple cell types. Spheroids can be formed using different techniques including, hanging drop culture, culture in ultra-low adhesion well plates and microarray culture [44]. When a spheroid is formed it can be introduced into a scaffold or hydrogel to allow for more freedom and vascularization of the tissue. Spheroid culture has been shown to improve the angiogenic effect compared to suspension cultures [45].
One of the most common approaches is to use a 3D scaffold to support cells in a static or dynamic environment, there the scaffold can positively affect the cell differentiation, migration and vascularization to form the desired tissue [43]. In general, the requirements for a good 3D scaffolds are biocompatibility, biodegradability and corresponding mechanical properties to the tissue [43, 46]. Because the natural ECM in the bone comprises a combination of organic and inorganic materials, it would be desirable to mimic this as close as possible. However, this can also be achieved by allowing the cells to produce a large amount of this ECM themselves. For bone a scaffold with HA would be the most obvious choice because it is the primary inorganic component of the ECM. However, HA is a solid, which limits its use for microfluidic setups since the cells and the scaffold must injected into the microfluidic device. It can however be supplemented in the particle form to improve the production of the bone matrix by the cells [47]. Different kinds of synthetic and organic solid scaffolds have been successfully used to mimic the bone (marrow) tissue in 3D [43].
Hydrogels are another commonly used matrix to mimic the physiology of a tissue *in vitro*. Hydrogels are typically cross linked polymer networks, they have similar structures and components to the actual tissue and are biocompatible. Hydrogels can be produced from natural and synthetic polymers, which allows for the customization of a wide range of properties to mimic the natural structure. For example, the stiffness and cross-linking methods can be customized to fulfill the desired needs. There are different organic hydrogels like; fibrin, matrigel, gelatin, HA, and collagen, and synthetic hydrogels like; gelatin methacrylate, polyethylene glycol and polyvinyl alcohol, that are used for biomedical applications. Cells can be cultured directly in the hydrogels and supplemented with drugs or growth factors that are slowly administered to the tissue. Hydrogels are especially interesting because they can be injected as a liquid phase and allowed to polymerize in a microfluidic channel. Like HA, the natural ECM of bone has a high concentration of Collagen I, which makes it a representative scaffold for this tissue. Different combinations of hydrogels have also been used to improve the characteristics for the specific culture [48]. Hydrogels can also be used in combination with assembled cell structures like spheroids. This will allow for the migration of the cells from the spheroids once seeded in the gel, instead of cells organizing from a dispersed state in the hydrogel. In Figure 1.3 a schematic representation of a scaffold, hydrogel and spheroid into which cells can be cultured are shown.
The structure into which a bone marrow model is formed must also be supplemented actively with nutrients and oxygen. Different approaches are again employed but the main two are a culture in either a bioreactor or microfluidic device. A conventional bioreactor comprises a big medium compartment where the biological structure is placed in. Through stirring and addition of supplements a dynamic environment is created, which can be monitored. Using a microfluidic device the bioreactor approach is minimized which allows for a more precise control of stimulation and

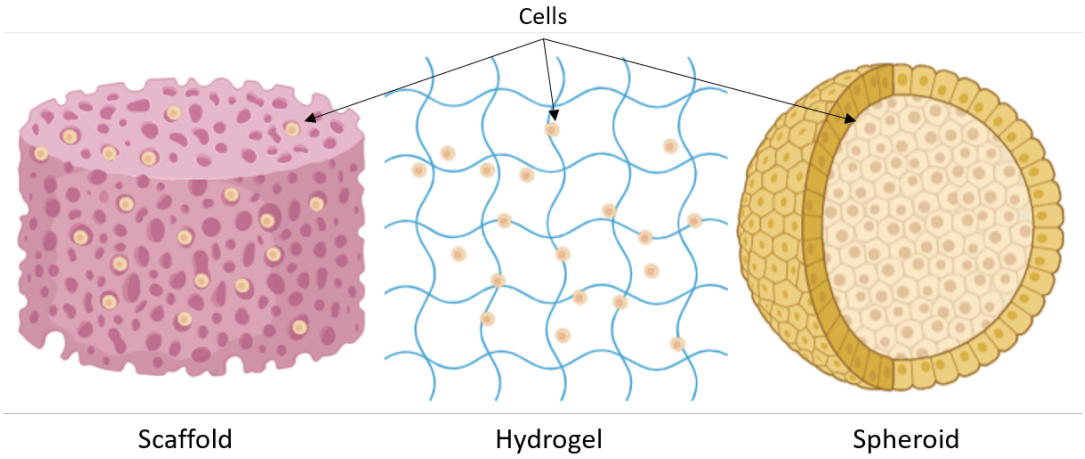

Figure 1.3: Example of three different 3D bone model approaches. Firstly, a solid scaffold in with cells are seeded. Secondly, a polymer hydrogel into with cells are seeded before it solidifies. Lastly, a spheroid culture of the cells. Created with BioRender.com

monitoring.

1.3.2 Microfluidics

To investigate the mechanisms of tumour metastasis, conventional 2D *in vitro* cultures or *in vivo* animal models have been primarily used in the past. On one hand, 2D culture has been used due to their cost effective materials, simple technologies and reproducibility [49]. However, these models lack the ability to replicate the full 3D microenvironment of the tissue [50]. On the other hand, *in vivo* animal models, mimic the physiological environment better, but lack human cells which limits the relevance for human response models [51]. 3D microfluidics have been introduced as a tool to mimic the physiological microenvironment of human tissue *in vitro* [4, 52]. Microfluidics allows for the accurate manipulation of liquids using channels in the micrometer scale, provides precise control of the stresses and (chemical) gradients perceived by different areas of the tissue in these devices, which is impossible in macro scale models and uncontrollable in *in vivo* studies [50]. Using a microfluidic approach, devices called OoC can be created; these devices or platforms mimic the functions, interactions and environment of a specific organ or cascade of organs. OoC have been in particular interesting for disease modelling and therapeutic development, and might eventually be combined to form a human-on-chip model [53]. Microfluidic devices are predominantly produced out of PDMS using soft-lithography [54]. The negative mould that is used for soft-lithography can be produced is different methods like photo-lithography and using 3D printers.

1.3.3 Vascularization on chip

To ensure proper growth and natural development of a tissue, vasculature is very important. New vasculature is formed by a process called angiogenesis, in which a new vessel sprouts from an existing one toward the site where this is necessary [55]. Especially for cancer this is an important process, which facilitates the oxygen and nutrient supply to tumour cells that are too distant from the original blood vessel, which is essential for survival and proliferation of these cells[56]. Endothelial cells and pericytes form the basis of the vessel lining; endothelial cells can be activated to perform angiogenesis by different angiogenic cytokines such as; vascular endothelial growth factor and fibroblast growth factor [55]. Thereby new vessels can be formed through the tissue to supply it with necessary nutrients and oxygen. Co-culture with fibroblasts is often used to promote antagonises because they secrete these angiogenic factors [57].
There have been various approaches to achieve vascularization *in vitro*; however until the use of microfluidics there had not been much improvements, this has allowed for much better control of the microenvironment [58]. For the existing vasculature to perform angiogenesis the endothelial cells should be able to migrate into the target tissue. To induce this will differ depending on the targeted organ, the chip design and the tissue matrix. Various of these microfluidic approaches have

been reported to achieve vascularization. In Figure 1.4 three different approaches are shown.

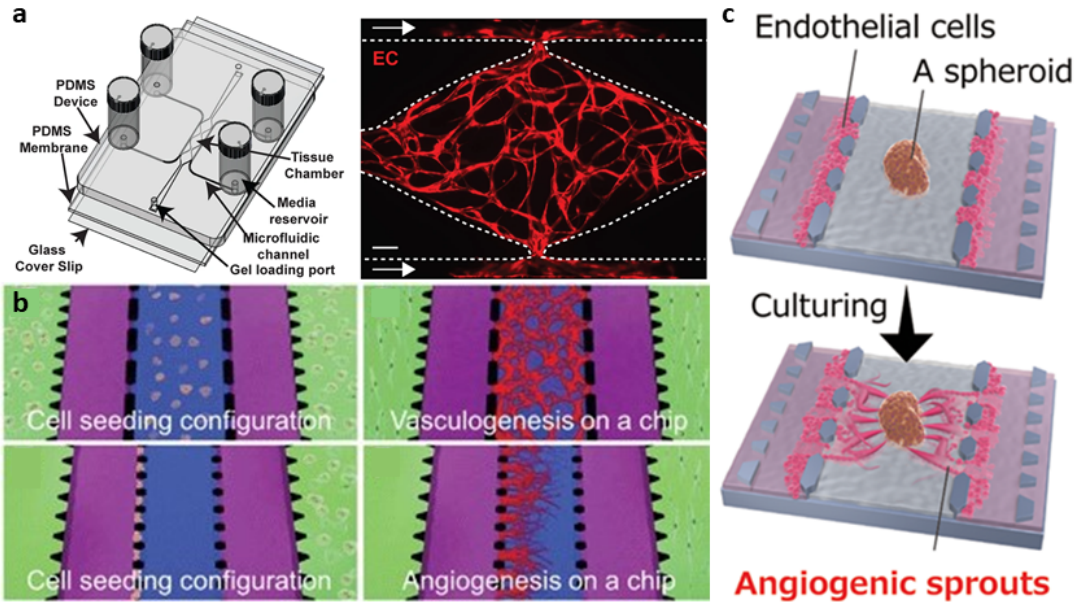

Figure 1.4: Three vascularization approaches where different layouts and cell structures are used. (a) Co-culture of ECFC-ECs and NHLFs as a suspension to form a vascular network that can support a micro-tumour formation. (b) A self assembly from suspension and sprouting approach to form vascularization. (c) Co-culture of NHLFs and HUVECS as a spheroid to and from which vascular sprouting is performed by the HUVECs. Adapted from [59, 60, 61].

Sobrino et al. displayed a microfluidic device to culture micro-tumours (Figure 1.4a) [59]. In this device ECFC-ECs and NHLFs where co-cultured in a 10 mg/mL Fibrinogen hydrogel suspension to form a vascularized network that can be supplemented with different cancer cells to study the micro-tumour formation. The central diamond shaped chamber is used for the tissue culture and the side channels for nutrient supply. After seven days of culture a vascular network was formed that was able to support the micro-tumour. Because the ECFC-ECs and NHLFs where cultured as a suspension no sprouting occurred from a vascularized channel, but the cells organized themselves in the hydrogel.
Kim et al. presented two different approaches to achieve vascularization using cell self assembly or sprouting (Figure 1.4b) [60]. Both approaches are performed in a 2.5 mg/mL Fibrinogen 0.2 mg/mL Collagen I hydrogel. Firstly upper row, HUVECs where cultured in a central chamber and NHLFs in the outer most chambers, with a medium channel in between. Using this configuration, the vasculature that connects the two media channels is formed by self assembly. Secondly lower row, the NHLF whereonly cultured in the most right chamber and the HUVECs on the side of the left medium channel. Thereby the endothelial sprouting into the hydrogel towards the factors secreted by the NHLF was determined.
Nashimoto et al. demonstrated a similar approach (Figure 1.4c). However, instead of a cell suspension a spheroid was used [61]. A spheroid containing NHLFs and HUVECs, was cultured in a hydrogel composed of 2.5 mg/mL Fibrinogen supplemented with 0.2 mg/mL Collagen I in a central chamber. On both sides of the culture chamber endothelial cells seeded that could form a vasculature into the culture chamber.
In the media channels endothelial cells can be seeded to mimic a blood vessel like structure. For this different approaches have been employed, as described in section 1.3.3 and in Figure 1.5. To form a lumen into which the endothelial cells can be seeded a technique called VFP can be used [58]. This technique will form a circular lumen through a hydrogel by passive pumping and relies on the displacement of a more viscous fluid by a less viscous one [62]. In the examples above the most common endothelial cells type that is used for the formation of the endothelial layer are HUVECs, however to mimic a specific tissue more accurately tissue specific endothelial cells can be used. As mentioned, the main component for vascularization is endothelial cells that are either cultured in a hydrogel suspension or layered on the side of a channel. This channel should be close to the tissue of interest to allow the endothelial cells to enter the tissue and form

new vessels; this is mostly achieved by separating the endothelial and tissue channel with pillars or small inlets. This allows for the separate ”seeding” of the channels but exchange after.

1.3.4 Metastasis-on-chip

Cancer metastasis is being extensively studied using different microfluidic platforms. Due to the complex cascade of events, as mentioned in section 1.1.1, studying metastasis requires a controlled environment, metastatic cascade different microfluidic devices have been developed to separately investigate the mechanisms. These separate components include tumour growth and intravasation, circulation, extravasation and colonization. When these steps are coupled together a complete primary-to-metastasis platform is formed. The main focus of their work is on the development of secondary tumour, so the circulation, extravasation and colonization are the most relevant steps. In Figure 1.5 different devices developed to study the circulation, extravasation and colonization are presented.

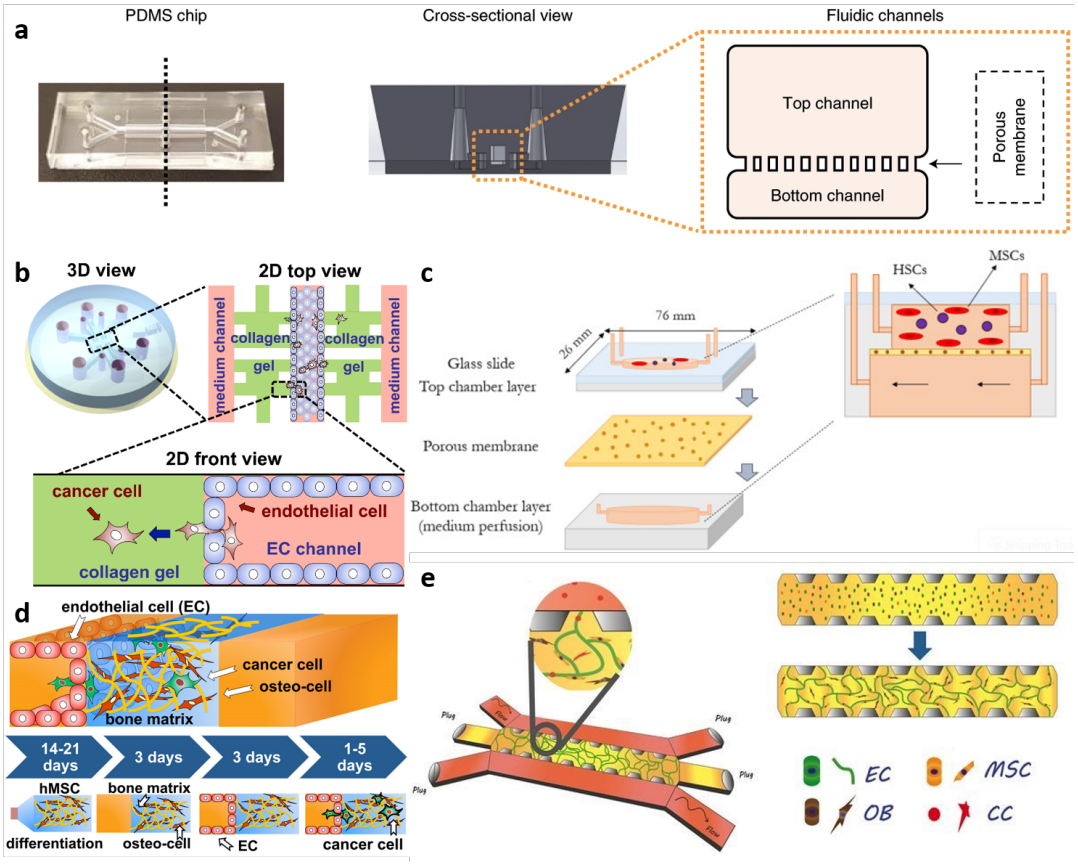

Figure 1.5: Different approaches towards the tissue formation where a and c have a stacked and b, d and e a side by side approach. (a) Co-culture of MSCs and HSCs in Fibrin hydrogel to from a functional bone marrow for investigation of bone marrow defects. (b) Model with a endothelial vessel through which tumour cells can extavasate into a hydrogel that models the extracellular space. (c) Mimicking of the bone marrow stromal niche with MSCs in a Collagen I hydrogel after which HSCs can be introduced to from a functional bone marrow for the investigation of multi-organ autoimmune diseases. (d) Culture of OBs differentiated MSCs in a Collagen I hydrogel lined with HUVECS to investigate the extravasation of breast tumour cells into the bone. (e) Co-culture of MSCs, OBs and HUVECs in a fibrin hydrogel to investigate drug treatments for the prevention of breast tumour to bone metastasis. Adapted from [63, 64, 65, 66, 67].

For the circulation and extravasation, the main structure is a chamber into which the desired tissue is formed, mostly called culture chamber. Next to the culture chamber nutrient supply is needed towards the cells which is provided by media channel(s) that can be oriented in different ways. In some designs the culture and media channels are side by side and in others the culture chamber is located on top of the media channel. When the channels are side by side, a design with one

central culture chamber and two media channels on its sides is primarily used, as illustrated on Figures 1.5b, 1.5d and 1.5e. For the stacked approach, the culture chamber is located on top of one media channel, as shown in Figures 1.5a and 1.5c. To allow for nutrient delivery, the culture and media channel are separated by a porous structure which can be pillars, that are incorporated in the microfluidic layer, or by placing a porous membrane in between. For the side-by-side design pillars are mostly used and for the stacked structure a porous membrane, due to the fabrication process. Both channels are accessible from a inlets and outlets through which cells can be injected and can be connected to a microfluidic setup. To form the tissue in the culture chamber, the desired cells are injected in a hydrogel as a suspension or as a spheroid after which the hydrogel is allowed to cross link to form the final 3D structure.

Bone Marrow on chip

Apart from the structural differences, the approach towards the tissue formation also differs between different designs. Chou et al. presented a platform for the investigation of bone marrow defects. In the top channel $CD34^+$ cells (HSCs) and MSCs are co-cultured in a Fibrin hydrogel to form the bone marrow tissue, and in the bottom channel HUVECs are seeded to form a complete endothelial lumen. After 2-4 weeks of culture the platform supports the differentiation and maturation of multiple blood cell lineages. This functional bone marrow was then exposed to different stimulations to simulate injury and allowed to recover using drug stimulation.
Kefallinou et al. showed a similar approach in which they mimicked the bone marrow stromal niche by culturing MSCs in a Collagen I hydrogel [65]. After 8 days they showed that the MSCs from multiple layers and organize themselves in a 3D structure. In the ongoing work they are planning to culture HSCs as well after a 8 day culture of MSCs to achieve a desired organization. Thereafter, the system, will be used as a platform to study systemic lupus erythematosus, a multi-organ chronic autoimmune disease.
Bersini et al. presented a human breast cancer metastases to bone platform in which they differentiated MSCs to OBs and measured the extravasation of of breast cancer cells into the tissue with the blocking of CXCL5 and CXCR2 [66]. The MSCs are seeded as a suspension in a 6 mg/mL Collagen I hydrogel and differentiated into OBs over two to three weeks. After differentiation a monolayer of HUVECs is added on the side of the bone tissue. Overall, they showed that CXCL5 and CXCR2 play a pivotal role in the breast tumour extravasation and that micro-metastases are formed in the bone tissue.
Jeon et al. showed a similar approach in the screening for drug treatments in the prevention of breast to bone metastasis [67]. MSCs, OBs and HUVECs are co-culture as a suspension in a 5 mg/mL fibrin hydrogel after which breast cancer cells are introduced. To promote the vascular network formation the inlets and outlets of the device are plugged except for two on the opposite side channels to generate interstitial flow through the tissue. Also, the effect of blocking the breast cancer A_3AR antagonist and anti-metastatic role of adenosine was investigated on the extravasation.

1.4 Aim and objectives

1.4.1 Aim

This MSc assignment is part of the CHIP-ME project whose aim is to replicate the metastatic cascade that is facilitated by various biological cues as depicted in Figure 1.6. To achieve this a circulation setup and tissue compartments for a breast to bone metastasis are developed. This can be distinguished in three separate components; the breast tissue in which a tumour is formed and from which CTCs are released, a circulation setup to establish inter organ communication and CTCs to and from the different organs, and finally a bone marrow tissue into which CTCs can form metastases. The project is therefore also conducted in these three separate components, and when all three are completed they are integrated into the platforms to form the breast to bone marrow metastasis-on-chip. This research project focuses on the development of the bone model.

Some research questions have been identified for the development of a bone marrow on chip. Firstly, what is the best approach to mimic a bone marrow tissue in a hydrogel using spheroids? Secondly, how can the generated bone marrow like tissue be vascularized? And finally, how

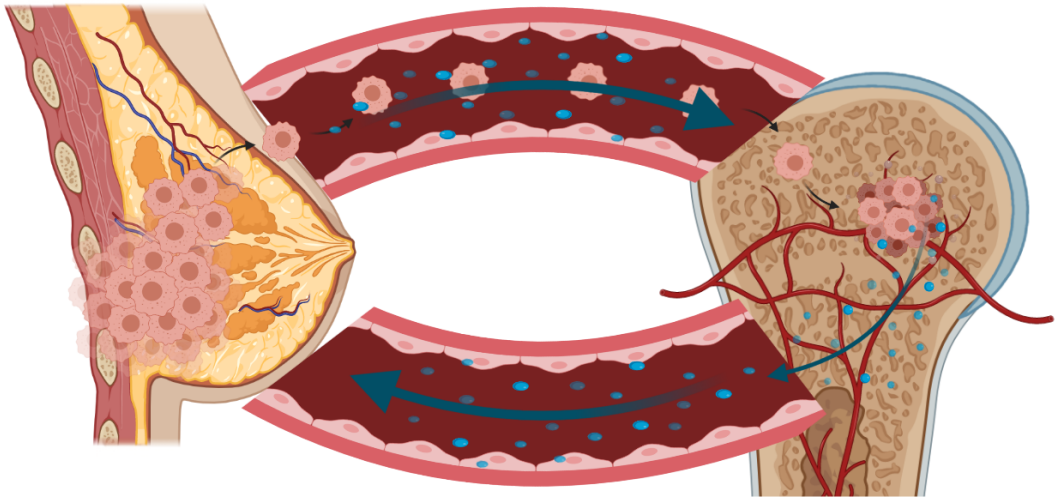

Figure 1.6: A schematic overview of the metastasis from breast to bone marrow tissue mediated inter organ communication that causes beast cancer CTCs to be attracted to the bone marrow. Created with BioRender.com

do different types of breast cancer CTCs interact with the bone marrow tissue to from (micro) metastases?

1.4.2 Objectives

To fulfill the aim and composed research questions the following objectives can be formulated. Firstly, the formation of spheroids based on cells that are present in the human bone marrow is optimized for;

- MSCs
- OBs
- ECs

And the optimal formation assessed using;

- Viability
- Morphology
- Culture criteria for extraction

Next, the selection of an optimal 3D matrix into which the formed spheroids are cultured. Two different hydrogels are considered;

- Collagen I
- Fibrin

And the effects on the spheroids using various imaging methods the cellular responses are analyzed and quantified in well plate cultures using;

- Viability
- Self organization by cellular migration

Now, the optimal spheroid composition has to be determined. For the best 3D matrix, spheroids with different cellular compositions are cultured in well plates and the following cellular responses quantified;

- Viability

- Protein production
- Self organization by cellular migration
- Gene expression

When the optimal 3D matrix and spheroid compositions are selected, these conditions are used for the on chip cultures. These conditions will be analyzed in the same manner as the spheroids cultures in well plates and compared to each other.
Separate to the bone marrow tissue optimization, the first steps into the formation of the vascular lumen comprised out of bone marrow specific endothelial cells will be performed.

2 MATERIALS AND METHODS

In this section the materials and methods, respectively, used and followed for the formation of the bone marrow on chip device. This includes the cellular cultures, the device fabrication, the microfluidic setup and the used analysis methods.

2.1 Cell culture

2.1.1 Routine cell culture

Bone marrow derived MSCs (donor 140B) were obtained from the hip bone marrow of a 77 year old male donor and cultured in α-MEM (Gibco) medium supplemented with 10% v/v FBS (Sigma), 1% v/v glutaMAX (Gibco), 1% v/v AsAP (Sigma) and 1% v/v pen/strep (Invitrogen). Human bone marrow derived endothelial cells were obtained from Celprogen and cultured in Human Bone Marrow Derived Endothelial Cell Complete Media with Serum (Celprogen). HUVECs were obtained from Lonzo and the culture medium was EGM-2 and 1% v/v pen/strep. RFP-tranfected HUVECs were obtained from PeloBiotech and the same culture medium as for regular HUVECs was used. Cells were cultured in culture flasks that were placed in a humidified incubator at 5 % CO_2 and 37 °C.

Cell removal and seeding

The confluent ($\approx$80 %) cells were washed with PBS, then trypsinized with 0.25% trypsin-EDTA (Gibco) for 3-5 min in the incubator, neutralized with medium and centrifuged at 300 g for 5 min. Next, the supernatant was aspirated, the cell pellet re-suspended in 1 mL of culture medium and the cell count estimated with a Hemocytometer [68]. Finally, a dilution was made to achieve the desired cell seeding density.

2.1.2 MSC differentiation

For the differentiation of the MSCs into Osteoblasts (OBs) the MSCs were seeded at a density of 5000 cells/cm^2 in a culture flask for 16 days; the differentiation medium comprises standard MSC culture medium with 100 nM of Dexamethasone (Sigma). To confirm the differentiation of the MSCs to OBs on day 16 a staining with Alizarin Red (Sigma) was performed and compared to a negative control. For Alizarin Red staining cells were fixed by first, washing them with PBS, then adding 4 % PFA and incubating at room temperature for 30 min at RT. Next, the PFA was removed and the cell layer washed 3 times with PBS. Alizarin Red was prepared by dissolving 1 g of Alizarin Red S in 50 mL of distilled water and adjusting the pH to 4.1 - 4.3 with NaOH. The Alizarin red solution was then filtered through a syringe filter with a 2 µm diameter pore size before adding it to the fixed cell layer. After 2 min of incubation at RT the Alizarin Red solution was removed and the cells washed three times with PBS.

2.2 Spheroid formation

2.2.1 Petri dish microwell array preparation

For the spheroid formation the MSCs were cultured in 35 mm diameter petri dishes in a microwell array prepared using hot embossing as described previously [69]. Shortly, a PDMS (Sylgard 184, Dow Corning) stamp prepared using a 5:1 w/w ratio with curing agent and presenting 49 pillars

of 600 µm diameter was used. The stamp was placed in the dish, pressure applied and the dish heated to 200 °C for 10 min and subsequently cooled down for 15 min to form the final dish with micro wells.

2.2.2 Pluronic coating

Before seeding cells in the microwell array, the petri dishes were cleaned thoroughly with 70% ethanol and coated with a 1% w/v Pluronic solution. The Pluronic coating was applied to prevent the attachment of the cells to the bottom and force them to form aggregates as described previously [69, 70]. The Pluronic solution was prepared by mixing 1 g of Pluronic power (Sigma) with 100 mL of Ultra pure water under magnetic stirring for 1 h and afterwards filtering it through a syringe filter with a 2 µm diameter pore size. 2 mL of Pluronic was added into each petri dish, centrifuged for 5 min at 300 g to remove air bubbles and incubated for at least 24 h before seeding of the cells.

2.2.3 Cell seeding

The cells were seeded in the microwell array with a total concentration of 2 million cells/petri dish. For the co-culture spheroids specific ratios of cells and medium were used, as summarized in Table 2.1. For the MSCs differentiated into OBs regular medium was used after differentiation in the spheroid cultures.
To force the cells into the microwells the petri dishes were centrifuged for 5 min at 300 g. Next, the cells that were not confined in the wells were flushed away by washing the dishes 3 times with PBS; afterwards, 2 mL of culture medium was added. The spheroids were next cultured for 2 days in the dish before experimentation.

Table 2.1: Cell and medium ratio's for different co-cultures

Co-culture	**Cell ratio**	**Medium ratio**
MSC-HUVEC	5:1	5:1
MSC-OB	5:1	-
MSC-BMEC	5:1	5:1
OB-BMEC	5:1	5:1
MSC-OB-BMEC	5:1:1	5:1

2.2.4 Viability staining

Viability staining of the spheroids cultured in petri dishes was performed after 2, 4, 7 and 10 days with Calcein AM and EthD-1 (Thermo Fisher) for live and dead cells respectively, to confirm the viability of the spheroids. A solution of 0.5 µL/mL Calcein AM and 2 µL/mL EthD-1 in culture medium was prepared, added to the petri dish and incubated for 30 min at 37 °C. The staining solution was flushed away by washing once with PBS and adding fresh PBS once more before imaging.

2.3 Spheroid hydrogel culture

2.3.1 Hydrogel preparation

Collagen I

Collagen I was prepared by diluting a stock Collagen I solution (Corning) with 10x PBS and 1 M NaOH solution to adjust the pH to obtain a final solution at 5 mg/mL with a pH of 7-7.5. The solution was kept on ice until further use to prevent it from solidifying and the pH measured using pH strips.

Fibrin

The Fibrin hydrogel comprises 2.5 mg/mL Fibrinogen (Sigma-Aldrich), 25 µg/mL Aprotinin (Sigma-Aldrich), 0.5 U/mL Thrombin (Sigma-Aldrich) and 0.2 mg/mL Collagen I. The Fibrin hydrogel was produced by preparing a solution of Fibrinogen and Aprotinin and a solution of Collagen I (prepared as described above) and Thrombin. The two solutions were mixed just before injection into the well plate or device to prevent premature solidifying.

2.3.2 Spheroid isolation from microarray

After 2 days of culture in the microwells the formed spheroids were ready to be isolated. The isolation was performed by pipetting over the microwells to dislodge the spheroids from the wells. Next, a single spheroid was collected with the micropipet with as little as possible culture medium.

2.3.3 Spheroid culture in hydrogel

Collagen I

A single spheroid was isolated, as described above, and pipetted into the Collagen I solution. Next, the spheroid was pipetted along with 100 µL of the Collagen I solution into a 96 well plate. The hydrogel was allowed to solidify for 15 min in the incubator at 37 °C after which 100 µL of culture medium was added. Medium was changed every other day.

Fibrin

A single spheroid was isolated and added to the Collagen-Thrombin solution. Next, the Fibrin-Aprotinin solution was added and, immediately after, the spheroid was pipetted along with 100 µL of the Fibrin solution into a 96-well plate. Hydrogel was allowed to solidify for 15 min in the incubator at 37 °C after which 100 µL of culture medium was added. Medium was changed every other day.

2.3.4 Viability staining

After 3, 5 and 7 days a viability staining was performed as described in Section 2.2.4, with an extended incubation time of 45 min to compensate for the diffusion into the hydrogel.

2.3.5 CellTracker

To evaluate the migration of the cells from the spheroids cells were stained with CellTracker dyes (Red and Green, Invitrogen). The desired cells were removed from the culture flasks in the same manner as mentioned in Section 2.1.1. The obtained cell pellet was mixed with culture medium without FBS and 10 µM of CellTracker Red or Green and incubated for 30 min. After incubation the staining solution was removed and the cells resuspended into their regular culture medium.

2.3.6 Immunostaining

To quantify osteogenic differentiation as well as other significant markers immunostaining for Osteocalcin, Phalloidin, VE-Cadherin, CD146, RNUX2 and DAPI was performed. Between the preparation and staining steps the cells were washed three times with PBS. First the culture medium was removed and the wells washed. Next, the cells were fixed with a 4% PFA solution and incubated for 30 min at RT. The fixed cells were washed and permeabilized with 0.25 % Triton X-100 for 30 min at RT. Blocking buffer of 1 % BSA was added and incubated for 1 h at RT after which the primary antibody for Osteocalcin, VE-cadherin, CD146 or RUNX2 were added at a dilution of specified by the manufacturers instruction in 1 % BSA buffer and incubated overnight at 4 °C.
After the primary antibody labeling the cells are washed and the secondary antibody (Alexa Fluor 488 or 647) was added at a dilution of 1:200 in 1 % BSA buffer and incubated for 1 h at RT. The cells are washed again and Phalloidin at a dilution of 1:400 in 1 % BSA buffer was added and incubated for 1 h at RT. The cells are washed again and DAPI at a dilution of 1:100 was added and incubated for 10 min at RT. The cells are washed a final time and PBS added for imaging.

2.3.7 Cell migration analysis

To quantify the amount of cellular migration into the hydrogel three different approaches have been considered using 2D projections of the spheroids;

- Manual amount limited to cells migrating the furthest from the spheroids center
- Rectangular plot profile of the gray scale through the spheroid core
- Spherical plot profile that measures the entire spheroid

These different methods are compared and optimal analysis method employed for quantifying the migration.

Manual migration analysis

To obtain a quantifiable measurement of the amount of migration into the hydrogel from the center of core of the spheroids of four cells that have migrated the farthest into the hydrogel is assessed. This was performed for three spheroids for every condition. In Figure 2.1, an example of such measurement is shown.

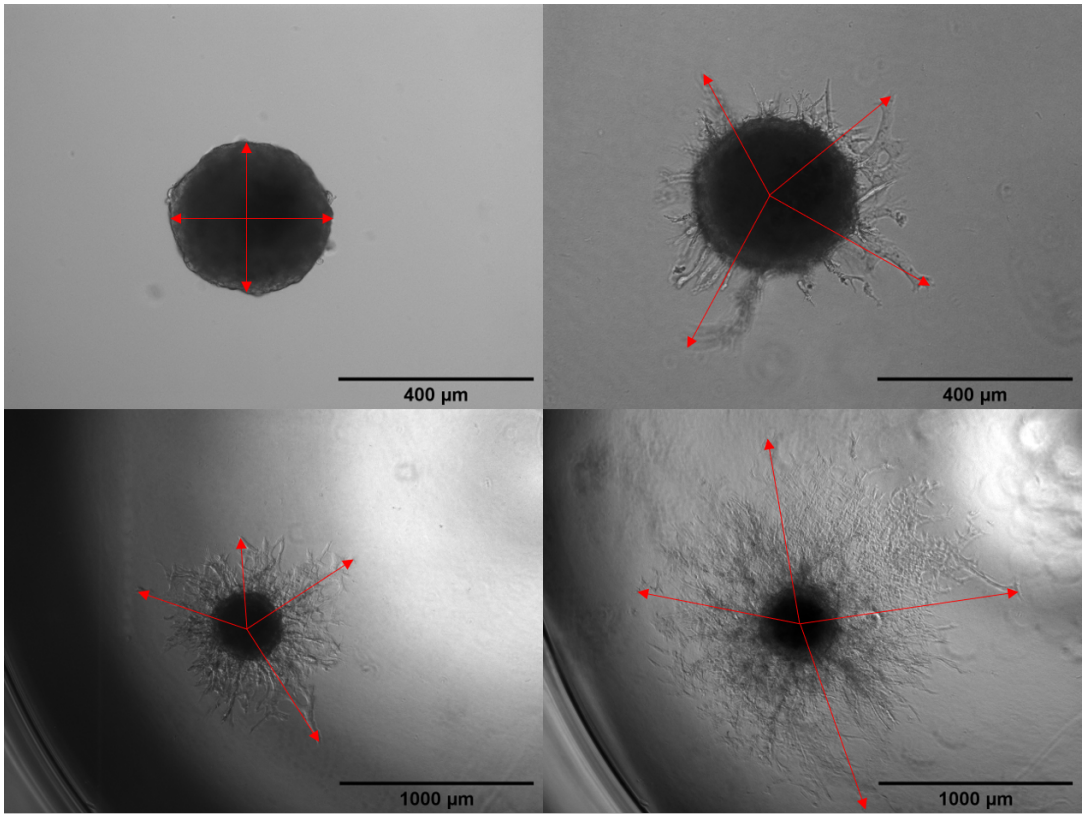

Figure 2.1: Measurements of the migration of cells from one spheroid on day 0, 3, 5 and 7.

Rectangular plot profile

For the rectangular plot profile a rectangle was drawn along the spheroid that covers the diameter of the spheroid core in ImageJ, as shown in Figure 2.2. Using plot profile analysis the gray scale was then calculated and the measurements normalized to the day 0 measurements to obtain graphs that show the trough at the same distance.

Spherical plot profile

The spherical plot profile was acquired in the same way as the rectangular plot profile only now using circle around the entire spheroids in ImageJ, as shown in Figure 2.3.

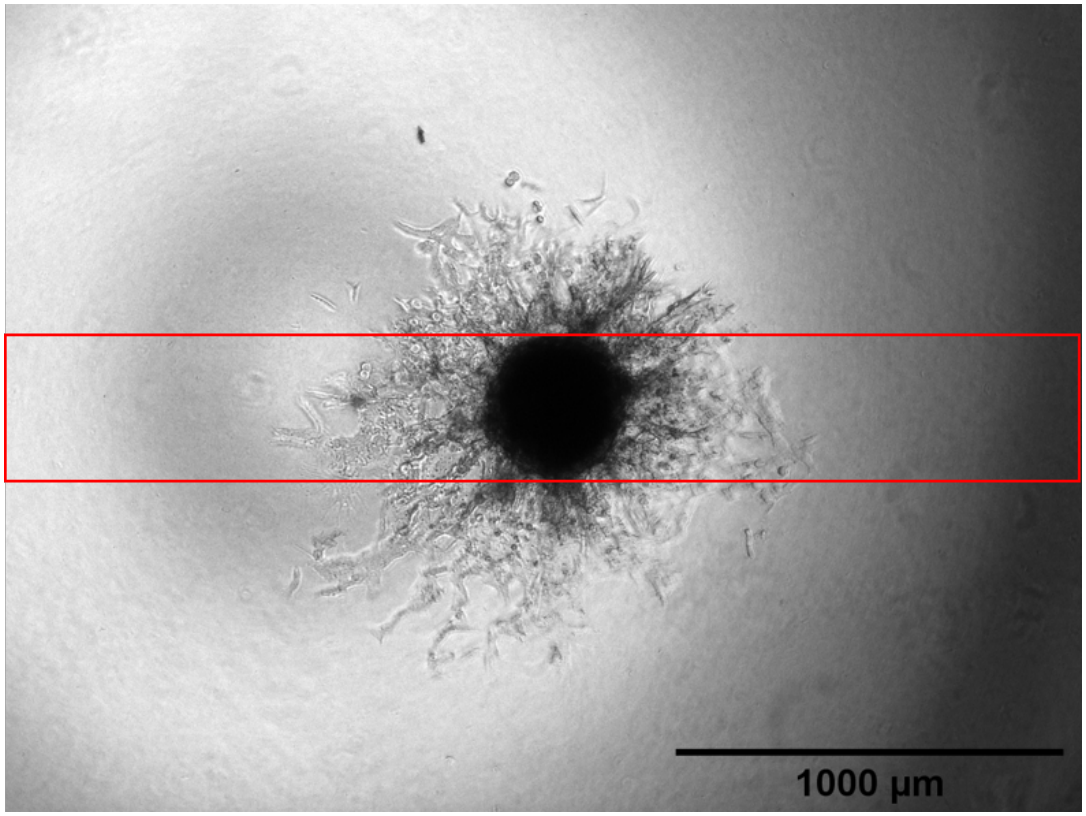

Figure 2.2: Measurement of the rectangular plot profile. The area inside the red rectangle is measured from left to right and the gray scale averaged.

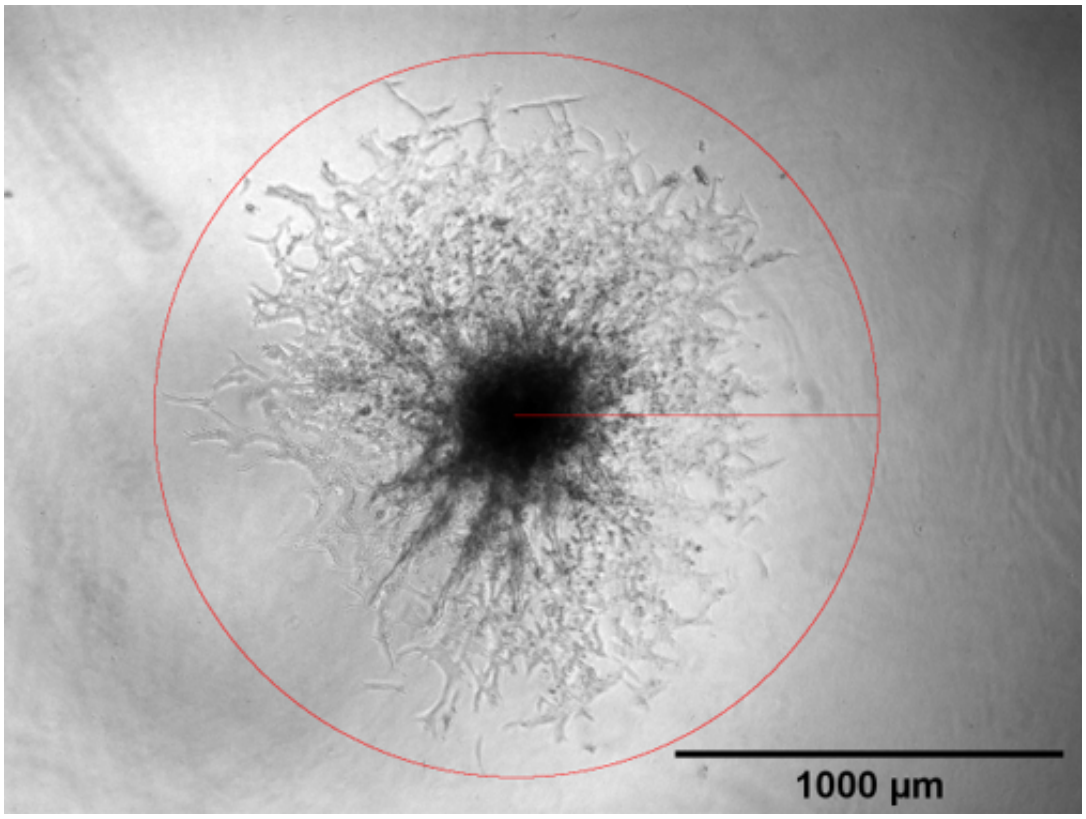

Figure 2.3: Measurement of the spherical plot profile. The area inside the red circle is measured from the center of the sphere towards the border and the gray scale averaged.

2.4 Microfluidic device

2.4.1 Design of the microfluidic device

The device comprises 5 different channels/chambers, as shown in Figure 2.4 along with detailed dimensions of the structures. One central culture chamber (green in Figure 2.4), two vessel channels flanking the culture chamber (blue in Figure 2.4), two additional perfusion channels on the other side of the vessel channels (yellow in Figure 2.4) and the channels and chambers are connected by small connecting channels (red in Figure 2.4). The height of the culture chamber and

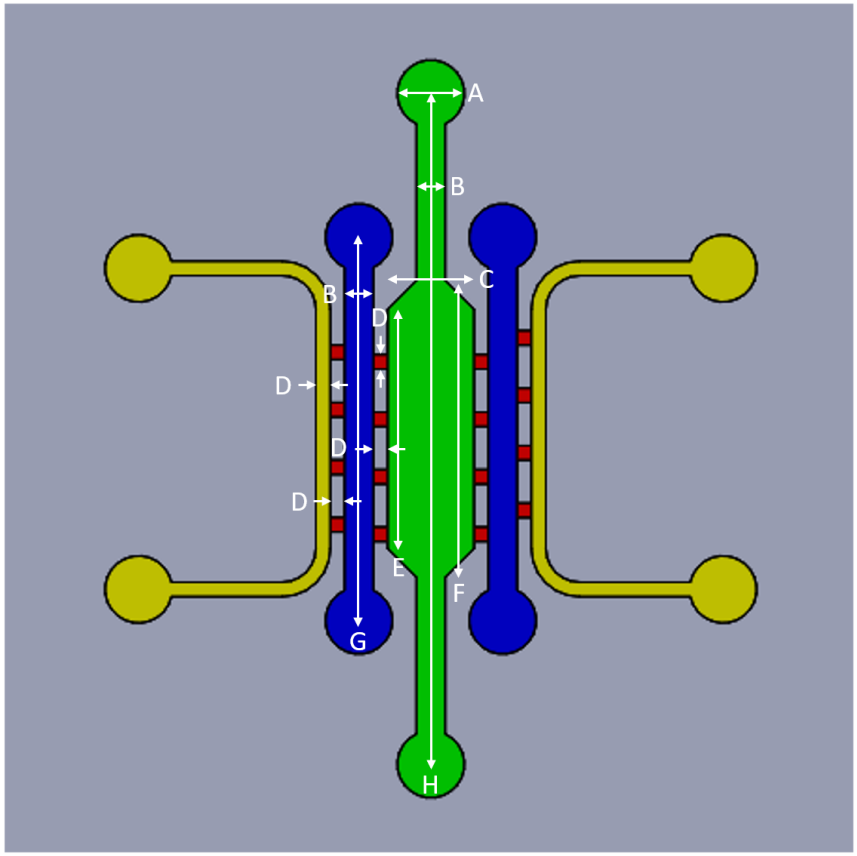

Figure 2.4: Layout of the device design with the following dimensions: A = 1.4 mm, B = 0.6 mm, C = 1.8 mm, D = 0.3 mm, E = 5 mm, F = 6 mm, G = 8 mm and H = 14 mm. Dimensions are to scale.

vessel channels is constant and equal to 0.6 mm, and the height of the additional perfusion channels and connecting channels is 0.3 mm. A design of the device was created using Solidworks software and imported into FlashDLprint software before 3D printing.

2.4.2 3D printing of the mould

The mould was created using a Flashforge Hunter 3D printer (Zhejiang Flashforge 3D Technology) with Fun-To-Do Deep Black resin. After printing the mould was washed quickly with acetone to remove excess resin from the mould, then washed with isopropanol and dryed with compressed air. Next, the mould was post-treated under 405 nm UV light with a power of 14 mW/cm^2 for 1 h and heated at 65 °C for 24 h.

2.4.3 Soft lithography

PDMS with a ratio of 10:1 w/w with curing agent, was mixed, degassed, and poured in the 3D printed mould. After a second degassing the mould was placed in an oven to cure over night at 65 °C. Next, the PDMS layer was extracted from the mould and the side with the fluidic features

covered with tape to protect it from dust. The inlets and outlets were created using 1- and 1.5-mm diameter punchers; 1.5 mm for the outlets of the vessel channels and 1 mm for all other inlets and outlets. The outlets of the vessel channels have a different diameter for VFP. Finally, the PDMS layer was oxidized using plasma treatment for 40 s at 50 W and 500 mTorr using a plasma oven (Cute, Femto Science) and bonded to a glass slide. The process of the mould and device fabrication is depicted in figure 2.5.

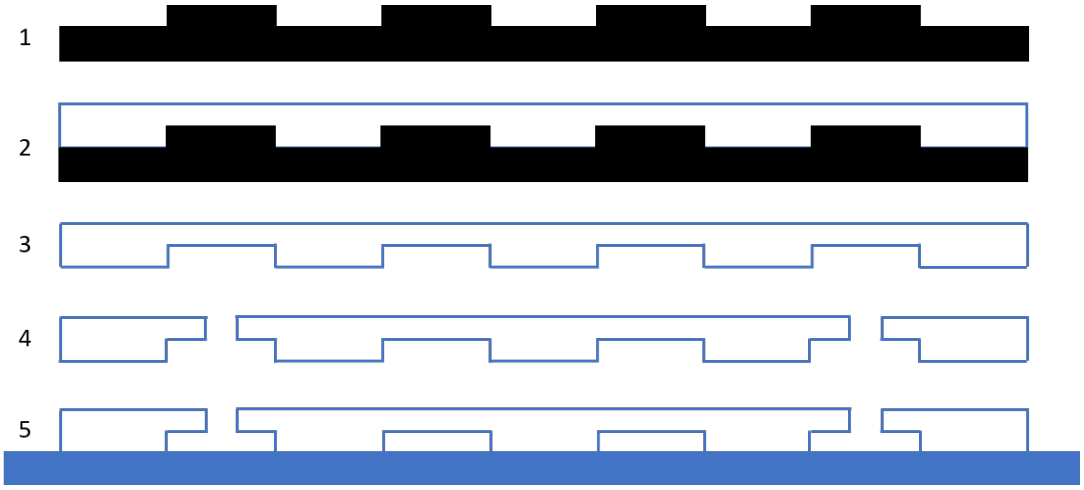

Figure 2.5: Schematic representation of the process of soft lithography to produce a PDMS microfluidic device from a 3D printed mould. 1: 3D printed mould, 2: PDMS is poured over the mould and left to cure, 3: The cured PDMS is extracted from the mould, 4: Inlets and outlets of desired size are punched into the PDMS, 5: The chip is bonded to a glass slide. Black = 3D mould, open blue = PDMS and filled blue = glass slide.

2.4.4 Chip preparation

After the chip has been fabricated the channels were functionalized to increase the wettability of the PDMS and ensure the Collagen I hydrogel would attach to the PDMS [71]. To this end, a 2 mg/ml polydopamine aqueous solution was prepared by mixing 2 mg of dopamine hydrochloride powder (Sigma-Aldrich) in 1 mL of TRIS buffer at pH 8.5. The solution was injected into all the channels, droplets placed on the inlets and outlets to avoid evaporation and the device incubated for 1 h at RT. Next, the channels were washed with MiliQ to remove the excess of polydopamine. Finally, the channels were air dried, washed with 70 % ethanol, air-dried once more and placed in an oven at 65 °C until further experiments. To inject the spheroids into a chip the same methodology as described in Sections 2.3.2, 2.3.1 and 2.3.3 was used. Except now 20 µL of Collagen I was taken up and injected into the culture chamber along with one spheroid.

2.4.5 Gene expression analysis

2.4.6 RNA extraction and cDNA production

The microfluidic chips were disassembled from the glass slide using a razor blade, the hydrogel with cells removed from the culture chamber and moved to an Eppendorf tube with 350 µL of Lysis buffer (Qiagen), to lyse the cells as well as the hydrogel, and stored at -20 °C. For cells cultured in the well plate, the hydrogel was extracted using a pipet and moved to the Eppendorf tube with 350 µL as well.
RNA was isolated from the hydrogel samples using the RNeasy Micro Kit (Qiagen), according to the manufacturer's instructions. RNA concentration and purity were determined using the NanoDrop 2000 spectrophotometer (Thermo Fisher Scientific). cDNA was obtained by reverse transcriptase of RNA, using the iScript cDNA synthesis kit from Bio-rad Laboratories (Bio-Rad) and the Bio Rad CFX Connect Real-time system (Bio-Rad).

2.4.7 qPCR

cDNA samples were diluted in RNAse-free water (Lonza) to obtain a final concentration of 5 ng/8 µL. Primers were prepared by diluting the forward and reverse primers in RNAse-free water. The primers and their sequence are listed in Appendix A.1. The diluted cDNA samples, SYBR reagent (SensiMix Bioline Reagents), and primers were loaded in a well plate. Analysis was performed using the Bio-Rad CFX Connect Real-time system (Bio-Rad). Obtained Ct values were normalized to the housekeeping genes to obtain ΔCt values.

2.5 Blood vessel formation

2.5.1 Viscous finger patterning

To form a lumen and eventually a blood vessel, the VFP technique was employed [62]. A Collagen I hydrogel solution was prepared in the same manner as explained in Section 2.3.1. Next, 10 µL of this solution was injected into the vessel channels, followed by pipetting 20 µL of culture medium on the larger outlet reservoir and, slowly, drops of medium onto the inlet reservoir. The less viscous culture medium flew through the center of the Collagen I in the channel, to create a lumen. The lumens were prepared one by one to avoid premature solidification of the hydrogel. The chips were next incubated for 15 min at 37 °C to finalize the polymerization of the Collagen I. The process of VFP is illustrated in figure 2.6.

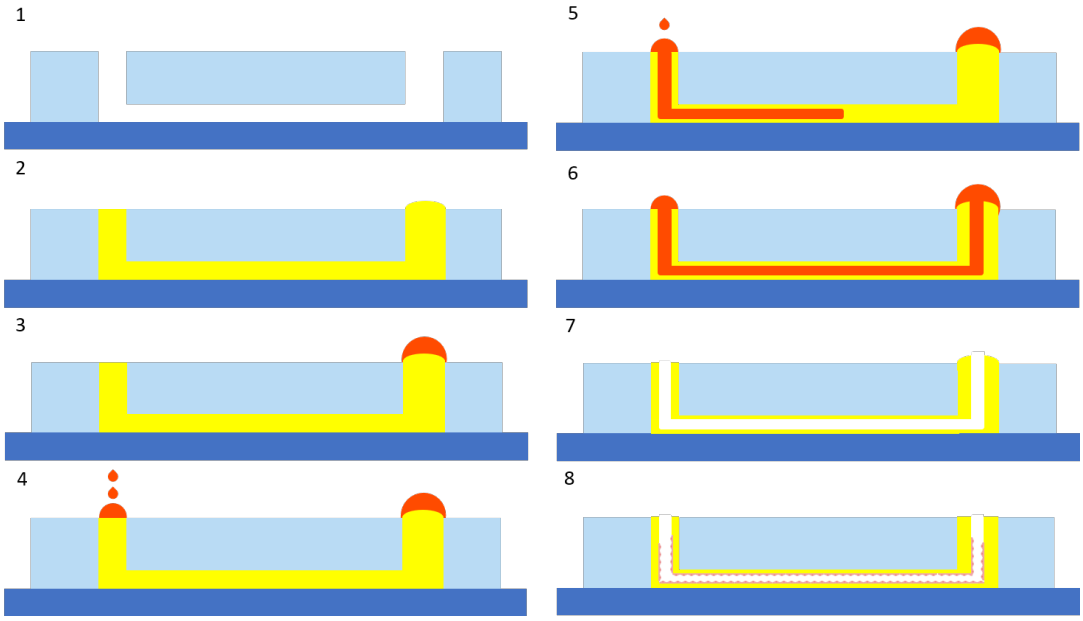

Figure 2.6: Schematic representation of VFP. 1: Cross section of a straight channel of the functionalized chip, 2: Hydrogel (yellow) is injected into the chip, 3: A large droplet of culture medium (red) is placed on the bigger outlet, 4: Small droplets of medium are pipetted on the inlet, 5: The small droplets flow through the hydrogel from the inlet to the outlet, 6: The medium has completely flown trough the Collagen and formed the lumen, 7: The final formed lumen when the medium is extracted, 8: Endothelial cells are seeded in the channel lumen.

2.5.2 Endothelial cell seeding

Next, bone marrow endothelial cells were seeded in the lumens. The bone marrow endothelial cells were prepared at a concentration of 10 million cells/mL. First, the channels were carefully flushed with culture medium and 5 µL of cell suspension was injected into the channel, and incubated for 1 h at 37 °C to seed the bottom of the channel. Finally, the top of the channel was seeded using the same method, after flipping the chip, and incubated again for 1 h.

VFP and the endothelial seeding was performed before spheroid injection to make sure that the lumens formed correctly. After both the lumen formation and spheroid injection, the final chip (cross section) of the device looks as depicted in Figure 2.7.

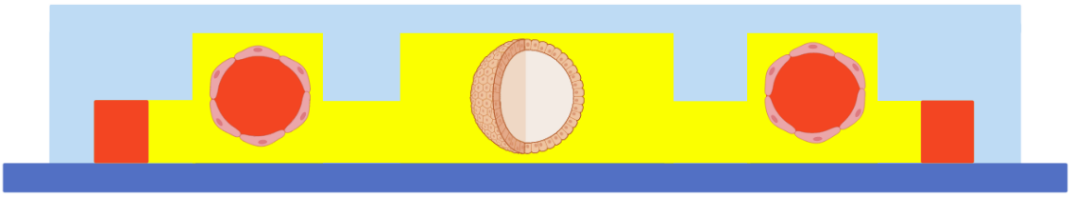

Figure 2.7: Cross section of the chip with a seeded spheroid in the culture chamber, two vascular lumens filled with culture medium (red) in hydrogel (yellow) in the vessel channels and external medium channels. Between the channels the connecting channels are visible.

2.6 Imaging

Imaging was performed with a EVOS M5000 microscope (Thermo Fisher) and A1 confocal microscope (Nikon). Filters used were: DAPI (Ex: 357/44 nm, Em: 447/60 nm), GFP (Ex: 470/22 nm, Em: 525/50 nm) , RFP (Ex: 531/40 nm, Em: 593/40 nm) and Cy5 (Ex: 628/40 nm, Em: 693/40 nm).

3 RESULTS AND DISCUSSION

In this section the results obtained from the experiments that are performed according to the Materials and Methods section are presented.

3.1 Timeline

Figure 3.1 summarizes the timeline of the experiments performed throughout the entire spheroid culture and which analysis was used and when. For the spheroids with OBs first a differentiation of 16 days was performed. Next, the spheroids were formed in the microwell arrays with the right cell ratios as shown in Table 2.1. After two days the formed spheroids are removed from the microarray and seeded in the hydrogel. Now, the spheroids are cultured for 7 days during which imaging is performed on day 3, 5 and 7 after which the cells are either fixed for immunofluorescence or lysed for qPCR analysis.

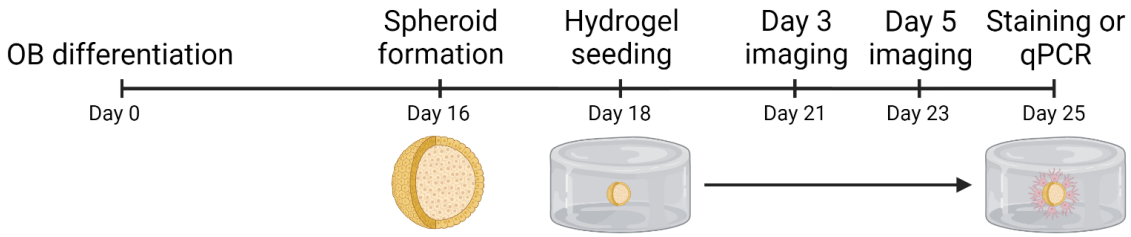

Figure 3.1: Timeline of the differentiation, spheroid formation, hydrogel culture and analysis. Created with BioRender.com

3.2 Spheroid formation and characterization

For the spheroids formation first the petri dishes with microwells are prepared. In Figure 3.2 an image of the microwell arrays formed using hot embossing (Figure 3.2A and B), as well as images focused on the inner diameter (Figure 3.2C) and outer diameter (Figure 3.2D) are shown. The outer diameter of the formed microwells is around 670 µm and the inner diameter around 250 µm.The outer diameter slightly larger than that the pillars in the PDMS stamp that is used in the hot-embossing are. This can be attributed to the expansion of the PDMS when heated or due to the deformation of the polystyrene when cooling down.
When cells were seeded they are well confined in the microwells and cells that were not confined properly are washed away. The wells are completely filled with cells, as can be seen in Figure 3.3. In Figure 3.3 the culture of MSCs in the microwells in shown up to 5 days. After one day cells started to adhere to each other and formed a spheroid. After two days the spheroids had not changed in shape significantly, which can again be seen in Figure 3.3. After 5 days the spheroid have shrunk a little bit; viability staining was performed which showed that the entire spheroid comprised only viable cells. The spheroids are cultured for different amount of days before extraction. After 5 days the spheroids were harder to remove from the microwells and due to the shrinking hardly visible with the naked eye. The difficulty of the spheroid removal could be due to the removal of the Pluronic coating of the wells after multiple medium exchanges or deposition of own ECM by cells. The removal of this coating allowed spheroids to attach to the bottom of the wells and prevented their dislodgement from the microwells. This problem was still present

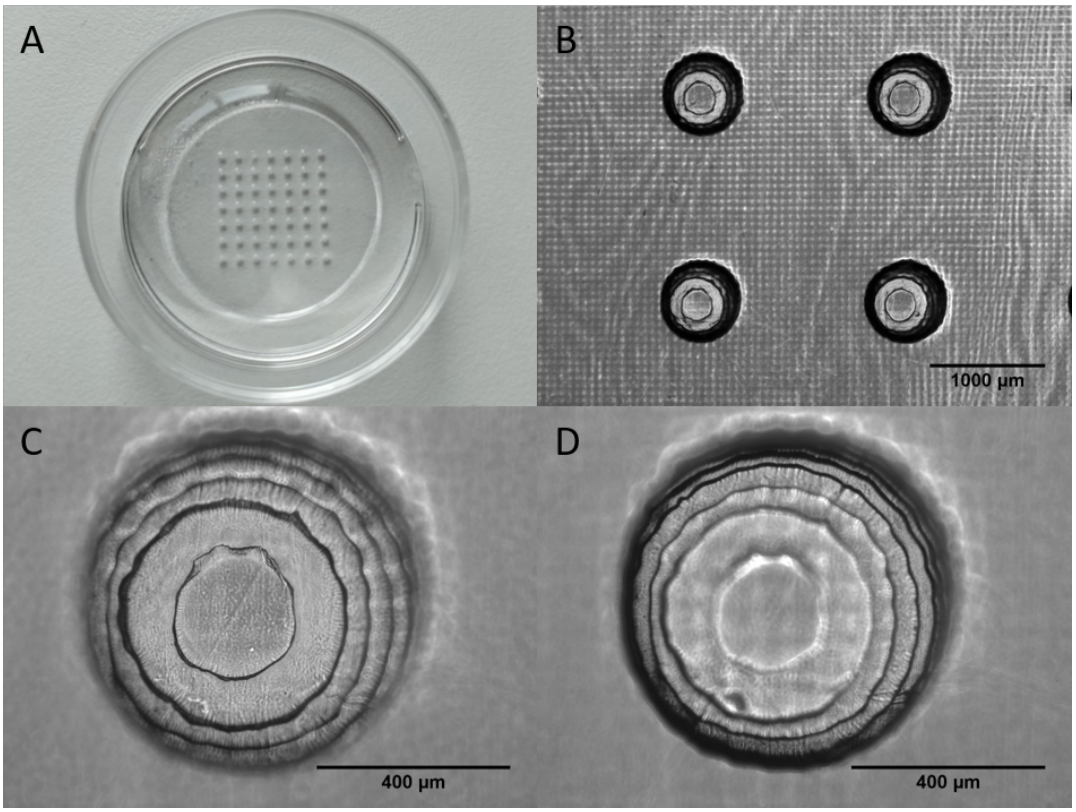

Figure 3.2: Macroscopic and microscopic image of the microwell array dish. (A) Marcoscopic image of the microwell array, (B) Microscopic image of multiple micro wells, (C) Zoom on the inner diameter of a single micro well, (D) Zoom on the outer diameter of a single micro well.

when the spheroids were cultured for 3 days. After 2 days of culture the spheroids were clearly visible with the naked eye and easy to dislodge from there microwells. So, two days of culture has been chosen as the microwell culture time after which the spheroids were removed from the plate and transferred into a hydrogel matrix. The spheroids were also cultured for longer times in the microwell to compare to the hydrogel, after 10 days the earlier round formed spheroid shrunk significantly and appeared to adhere to the bottom. This is most likely caused by the lack of adherence possibilities. However, the spheroids were still showing high level of viability with only some of the cells being dead.
Due to the washing away of the cells that were not confined in the microwells it is not exactly known how many cells are in one spheroid. When assuming that most of the cells were confined and from the final spheroid the cell density should be somewhat below the 40.000 cells/spheroid, however this is hard to confirm due to the high amount of cells.

MSC osteogenic differentiation

After the 14 day of culture staining with Alizarin red was performed to confirm the osteogenic differentiation. The Alizarin red stains the Calcium that is deposited by the OBs when differentiated from MSCs [72]. In Figure 3.4A the staining on differentiated OBs is shown. Also, the morphological changes after the differentiation culture can be noted as presented Figure 3.4B and C. These changes include the visible deposition of Calcium around the OBs, which can be seen in little amount in the undifferentiated culture due to differentiation into OBs caused by the higher density after 14 days of culture. Dexamethasone that was added to differentiate the MSCs to OBs forces cells in cell arrest, which stops the division of the cells. When MSCs were cultured at the same density for 14 days they do keep dividing until a too high density was achieved. This increase in density can also cause MSCs to differentiate into different lineages.

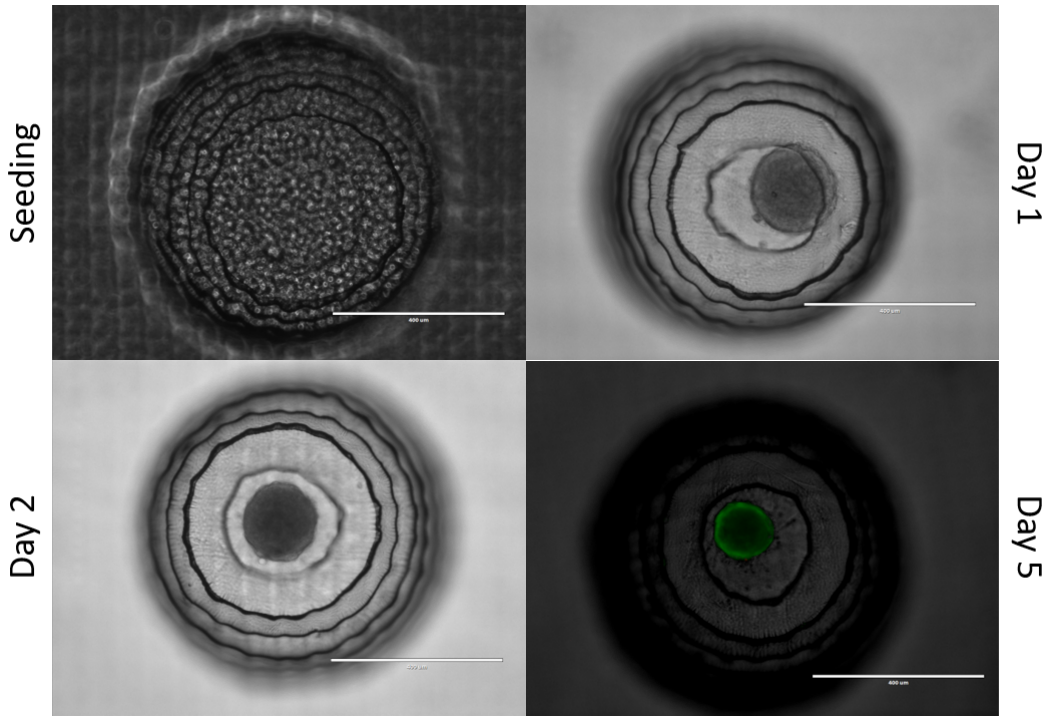

Figure 3.3: MSCs spheroid seeding in microwell array right after seeding, after 1 day, after 2 days and viability staining with Calcein AM and EthD-1 after 5 days. Scale bar indicates 400 µm.

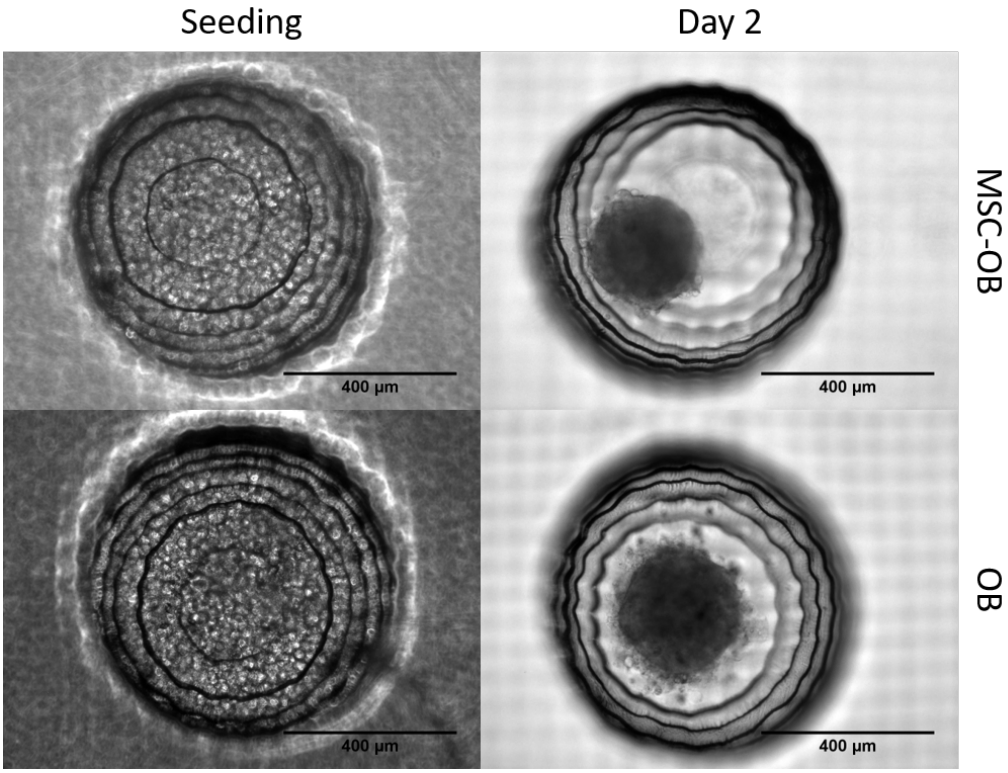

Figure 3.5: MSCs-OB (5:1) and OB spheroid formation in microwell array, right after seeding (left) and after 2 days (right).

When OBs are co-cultured with MSCs or employed for mono spheroid formation, they exhibited a different spheroid morphology (Figure 3.5); after 2 days they looked significantly different compared to the MSCs spheroids. The OB and MSC-OB spheroids had rougher outer surface com-

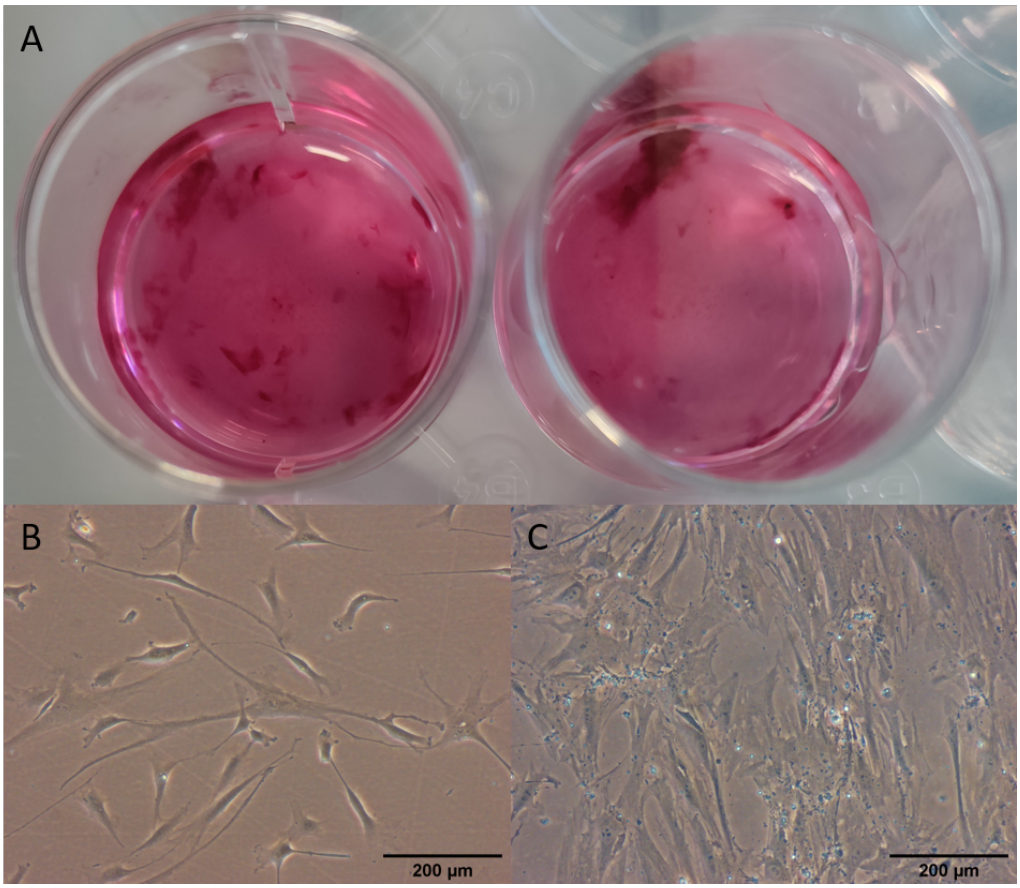

Figure 3.4: (A) Alizarin red staining on OBs differentiated from MSCs, (B) morphology of the MSCs in 2D culture, (C) morphology of OBs in 2D culture.

pared to the MSC spheroids. This has also been seen in previous publications, where spheroids with MSCs had a smooth outer surface [73], and spheroids with OBs included more round cells on the surface [74]. Apart from the morphological differences, the OBs and MSC-OB spheroids appeared to be slightly larger compared to the MSC spheroids.

3.3 Hydrogel culture

3.3.1 MSC spheroids

After two days spheroids were transferred into a hydrogel solution in a well of a 96 well plate. For both Collagen I and Fibrin hydrogels images of the spheroids are presented directly after being placed in hydrogel culture (Day 0) and after viability staining after 3, 5 and 7 days in culture (Figure 3.6). Zoomed out images of the spheroids in Fibrin hydrogel are shown in Appendix A.2 to show the total amount of migration of cells into the hydrogel. For Collagen I this was not necessary due to the lack of migration.
In the different images it can be seen that the cells in the spheroid are viable after 7 days of culture. For the Collagen I hydrogel the shape of the spheroids remains mostly the same after the culture up to 7 days and vesicles like structures are secreted around the spheroids cultured in a Collagen I hydrogel. Also, there is no significant change in the spheroid size visible up to 7 days. However, for the final tissue formation vascularization is required and it is preferable that this occurs from the spheroid as well as from the endothelial lumen. So, the migration of some of the MSCs is preferable which can not be seen for the Collagen I hydrogel.
For the Fibrin hydrogel the spheroid seemed to have decreased, which might be due to the spreading of MSCs into the Fibrin hydrogel. It is clear that the cells start to migrate from the spheroid after 3 days, this migration increased significantly towards day 7. Park et al. showed that a Fibrin-Collagen I hydrogel could promote vascular formation by HUVECs without gel retraction in

microfluidic platforms [75]. Also, Rao et al. investigated the effect of different concentrations of hydrogel in a Fibrin-Collagen I hydrogel on a vascular network formation [76]. They found that gels comprising only either of these two components showed a lower amount of vascular formation compared to a combination of the two. So, for both hydrogels the viability of the spheroid was good but a bit difference in the amount of spreading of the spheroid into the surrounding hydrogel was observed. Apart form the improved physiological effect of the Fibrin hydrogel, it can also be seen that imaging of the spheroid was easier than in Collagen I hydrogel. Images in Collagen I are distorted by the hydrogel itself and spreading cells were hard to identify through the hydrogel network. the Fibrin hydrogel was clearer which allowed better imaging of the spheroid. Also, spheroids in the Collagen I seemed to be producing vesicle like structures that could be extracellular vesicles or apoptotic bodies for example. However the exact origin still has to be investigated further.

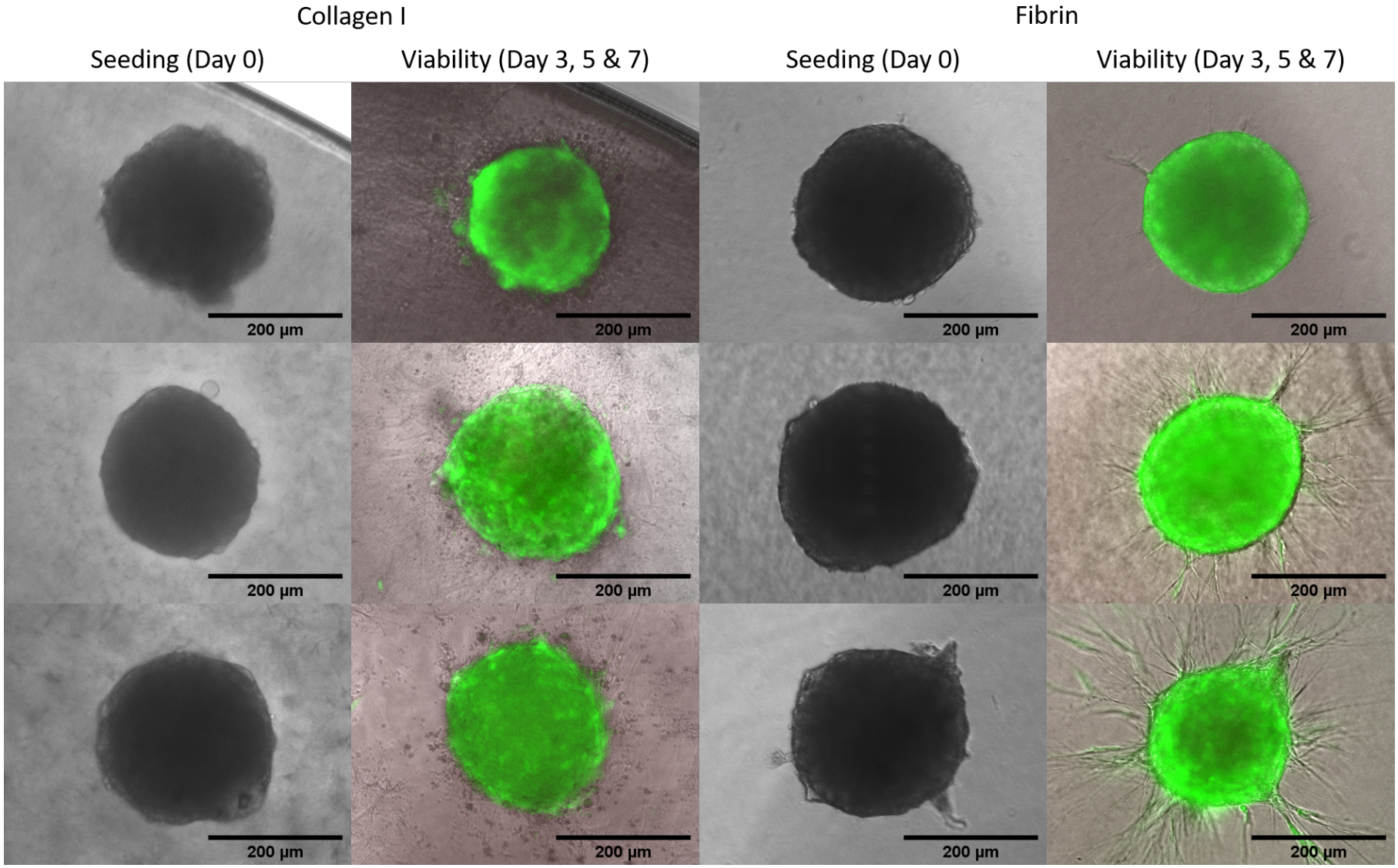

Figure 3.6: Spheroids cultured in a Collagen I (5 mg/mL Collagen I) and Fibrin hydrogel (2.5 mg/mL Fibrinogen, 25 µg/mL Aprotinin, 0.5 U/mL Thrombin and 0.2 mg/mL Collagen I) on day 0 and viability staining with Calcein AM and EthD-1 after 3, 5 and 7 days.

3.3.2 MSC-HUVEC co-culture spheroids

Rao et al. showed that a Fibrin-Collagen I hydrogel would produce a better vascular network compared to a Collagen I hydrogel [76]. Also, they used various MSC to EC ratios to optimize the vascular network formation after 7 days, and form that a 2:3 and a 5:1 ratios were the best. A 5:1 ratio was chosen in this work to be sure that there was enough of the desired tissue formed while still achieving vascularization.

MSC-HUVEC spheroids with RFP labeled HUVECs

The effect of a spheroid co-culture of MSCs with HUVECs was investigated using HUVECs that were transfected with RFP. HUVECs were added to try to increase the vascularization of the formed tissue. RFP-HUVECs were used to because this allows tracking their migration into the hydrogel. In Figure 3.7 overlays of the RFP fluorescence for the HUVECs after seeding and after day 3, 5 and 7 are shown in both Collagen I and Fibrin. Since HUVECs are red fluorescent no viability staining could be performed with these spheroids. In Figure 3.8 a separate MSC-HUVEC co-culture spheroid without fluorescent HUVECs was performed in hydrogel to confirm the viability. Zoomed out images of the spheroids in Fibrin hydrogel is shown in Appendix A.3 to show the total amount of migration of cells into the hydrogel. For Collagen I this was not necessary due to the lack of migration.
From the co-culture with fluorescent HUVECs it is visible that the HUVECs were not migrating and were only moving inside the spheroid, as the RFP signal was only present in the spheroid core on day 0 as well as after up to 7 days of culture. Also, it can again be seen that the spreading of the cells was much higher for the Fibrin hydrogel compared to the Collagen I hydrogel. But, also a clear difference was visible when comparing the Fibrin culture with and without HUVECs. When the HUVECs were present spreading from the spheroids appeared to be again higher compared to the spheroids with only MSCs. However, the cells that were spreading were not red fluorescent, so these were not the HUVECs but the MSCs that were spreading more (Figure 3.7). This shows that the presence of HUVECs influenced the amount of cellular spreading from the spheroids. This has also been reported by Heo et al. [77], that compared MSC and MSC-HUVEC co-culture spheroids in terms of cell viability, morphology, proliferation, and gene expression profile. They found that the co-culture of MSCs with HUVECs resulted in a increase of the cell spreading and proliferation, as well as an up-regulation in osteogenic differentiation and pre-vascular network formation.
Because these HUVECs are RFP labeled no viability staining with EthD-1 was be performed. Therefore a separate culture of MSCs with HUVECs that were not RFP labeled was used to assess the viability of these co-cultures. The separate co-culture without RFP labeled HUVECs in FigureA.4 shows that the viability of the spheroids in both hydrogels was good apart from some small amount of cell death visible in the spheroids after 3 days in Fibrin hydrogel. Due to the high viability in all measured spheroids it is now assumed that nutrient delivery and thus the viability in all other spheroid cultures is similar. Thus, there have been no more viability assessments of the further spheroid cultures. Zoomed out images of the spheroids in Fibrin hydrogel is shown in Appendix A.4 to show the total amount of migration of cells into the hydrogel. For Collagen this was not necessary due to the lack of migration.

Figure 3.7: Co-culture of spheroids with MSCs-RFP HUVECs (5:1) in a Collagen I and Fibrin hydrogel on day 0 and migration after 3, 5 and 7 days.

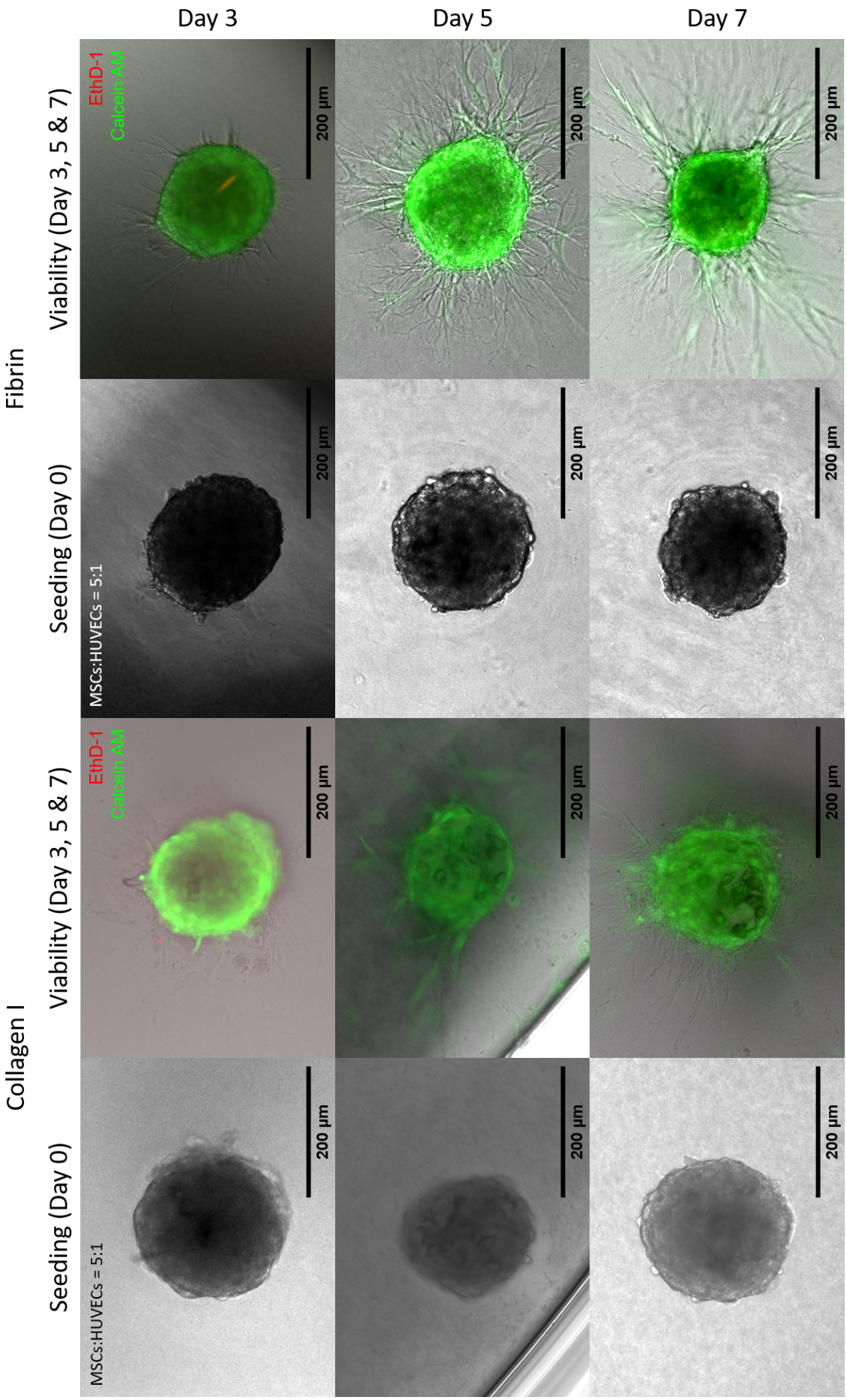

Figure 3.8: Co-culture of MSCs-HUVECs (5:1) spheroids in a Collagen I and Fibrin hydrogel, on day 0 and viability staining with Calcein AM and EthD-1 after 3, 5 and 7 days.

MSC-HUVEC spheroids with CellTracker

From the spheroid culture with RFP labeled HUVECs an increased migration of cells from the spheroids was observed especially for the Fibrin hydrogel. HUVECs appeared to stay inside the spheroids core. To confirm that indeed the MSCs were spreading, both cell types were stained with CellTracker Red (HUVECs) and Green (MSCs). CellTracker labels the cells with a fluorescent marker that remains in dividing cells. However the fluorescence drops compared to not dividing cells. In Figure 3.9 the migration of both cell types from the spheroid into both hydrogels is shown for the same spheroid during the 7 day culture. Most of the red and green fluorescence is overlapping in these images. However, it can also be seen that almost none of the cells that have migrated from the spheroid bear any fluorescence. This can be due to the fact that the fluorescence of the cells is reduced upon division or that the amount of fluorescence from the spheroid core is too high compared to the cells spreading into the hydrogels. From the culture with the RFP transfected HUVECs it can definitely be said that the HUVECs were not migrating into the hydrogel because their fluorescence is permanent even after cell division. So, combining the findings from both the RFP transfected and CellTracker stained cells, it is likely that the spreading cells from the spheroid are MSCs, due to the fact that the RFP from the transfected HUVECs are only visible in the core spheroid. As well as, that the cells are most likely dividing to be able to migrate from the spheroid, and due to the fact that the migrated cells do not bear a (strong) fluorescence signal.

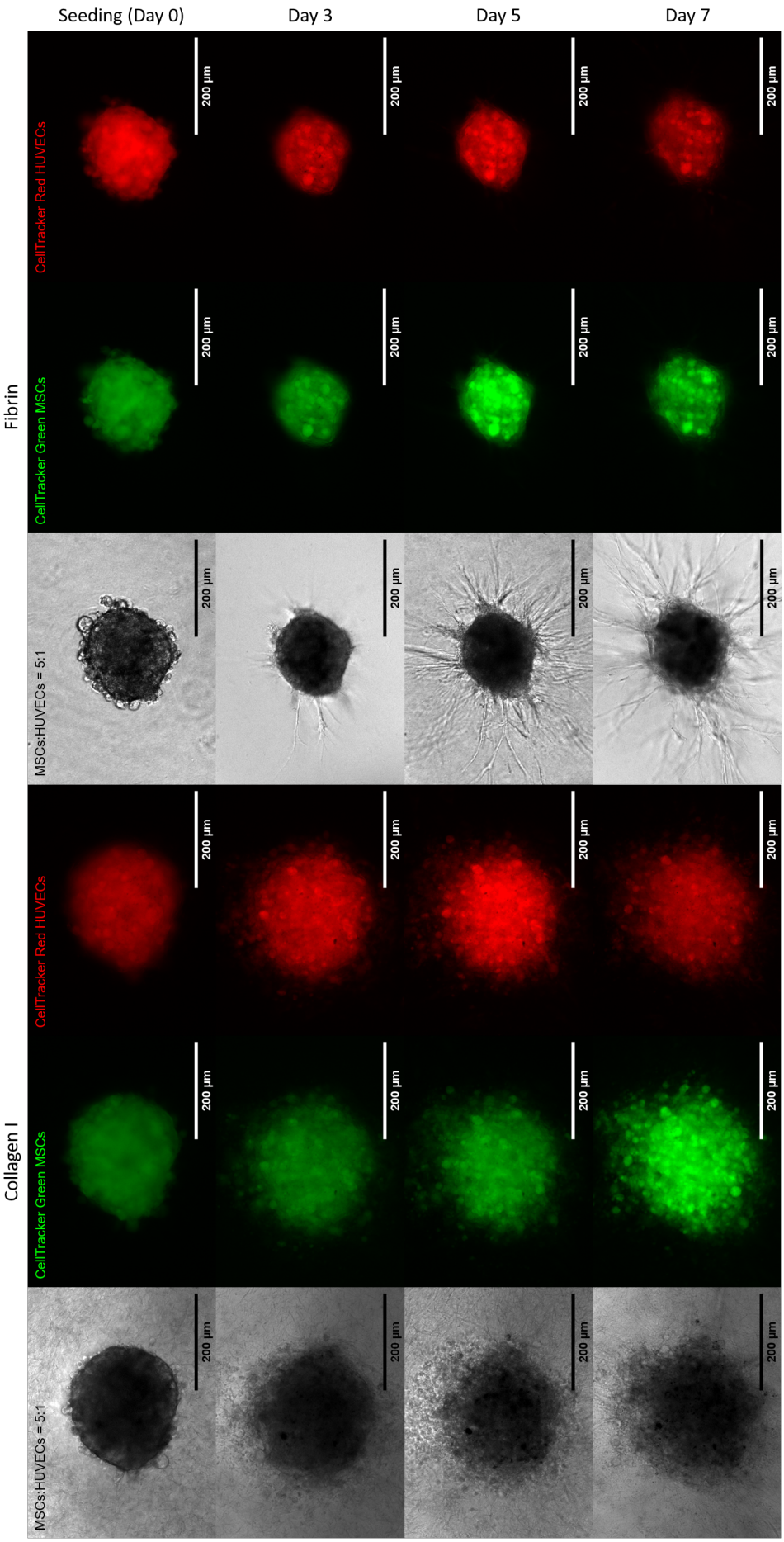

Figure 3.9: Co-culture of MSCs-HUVECs (5:1) spheroids stained with CellTracker Green and Red respectively, in a Collagen I and Fibrin hydrogel on day 0 and the migration of both cell types after 3, 5 and 7 days.

3.3.3 MSC-OB co-culture spheroids

Next, spheroids in combination with OBs were seeded in the same hydrogels to investigate the effect of the OB cells on the behavior in the hydrogel culture. The addition of OBs would add to the representativeness of the formed tissue compared to bone marrow. Sano et al. has previously reported that migration rates of breast cancer cells towards spheroids were significantly higher in a osteo-differentiated MSCs compared with to microenvironment formed by undifferentiated MSCs [78]. So, addition of the OBs should show an increase in the extravasation of the cancer cells into the bone marrow tissue. In Figure 3.10 co-culture of MSCs and OBs with a ratio of 5:1 and only OBs are shown in Collagen I and Fibrin hydrogels. This ratio is chosen similar to the MSC-HUVEC co-culture to get a similar ratio as in the bone marrow tissue, as well as enough MSCs that can still differentiate and form a more bone marrow-like tissue. Imaging of spheroids in Collagen I hydrogel is again difficult, still it was visible that there are some production or excretion of vesicle like objects around the spheroids. Also, there was no visible spreading from the spheroids into the hydrogel. In Fibrin the spheroids were again much better visible, with significant spreading into the hydrogel after day 3 but no significant increase up to day 7.
As a comparison also spheroids consisting only of OBs were seeded into the hydrogels as shown in Figure 3.10. The rougher spheroids that were formed from the OBs were still visible in the hydrogel, but here no spreading was visible in either of the hydrogels. There was however a small decrease in the spheroid size after day 3. In Fibrin there seemed to be some mineralization around the spheroid at day 7, this is not present in the MSCs-OBs co-culture which is probably produced by the OBs. This mineralization is visible at the border of the OB spheroids in at day 5 and 7 in Figure 3.10
After 7 days of culture cells were fixed and stained for Osteocalcin (Green), Phalloidin (Red) and DAPI (Blue) and imaged using confocal microscopy. A Z-stack was performed from the bottom till the top of the spheroid. This Z-stack was then reconstructed using ImageJ and a 3D and 2D image was then generated to obtain a total image of the fluorescence in the spheroids.
In Figure 3.11 images of the MSCs-OBs spheroid are shown in Collagen I and Fibrin hydrogels. From the cell nuclei that are stained using DAPI it can be seen that most of the cells were still in or around the spheroid. There seemed to be almost no migration of the cells into the hydrogels, because there were not much cell nuclei visible outside the core of the spheroids. In green the produced Osteocalcin is visualized in small amounts, which was produced by the OBs. There are other green fluorescence signals present around the spheroids, these are most likely some background noise or interference because they were not visible in the preliminary images but only appeared when a second imaging was performed. The remaining green fluorescence was only present in the core of the spheroids. The Phalloidin stains actin filaments that are present in the cells these were mainly present in the spheroid core, This also shows almost no migration from the spheroids. However, there was no clear organization visible from this actin staining.
When comparing the mono- to the co-culture spheroids it can be seen that there seemed to be a small increase in the Osteocalcin between the MSCs-OBs and OBs spheroids. This is most likely due to the higher concentration OBs that were present in the spheroids and shows that the OBs are producing the Osteocalcin. Apart from the limited amount of fluorescence outside the spheroids and the increase in Osteocalcin in the OB spheroids there were no significant differences between these spheroids.
Form the previous hydrogel cultures it was clear that the Fibrin hydrogel gave better characteristics compared to the Collagen I hydrogel, by means of better cellular organization and viability of the spheroids. Therfore, for the final well cultures and the chip culture only the Fibrin hydrogel was further considered.

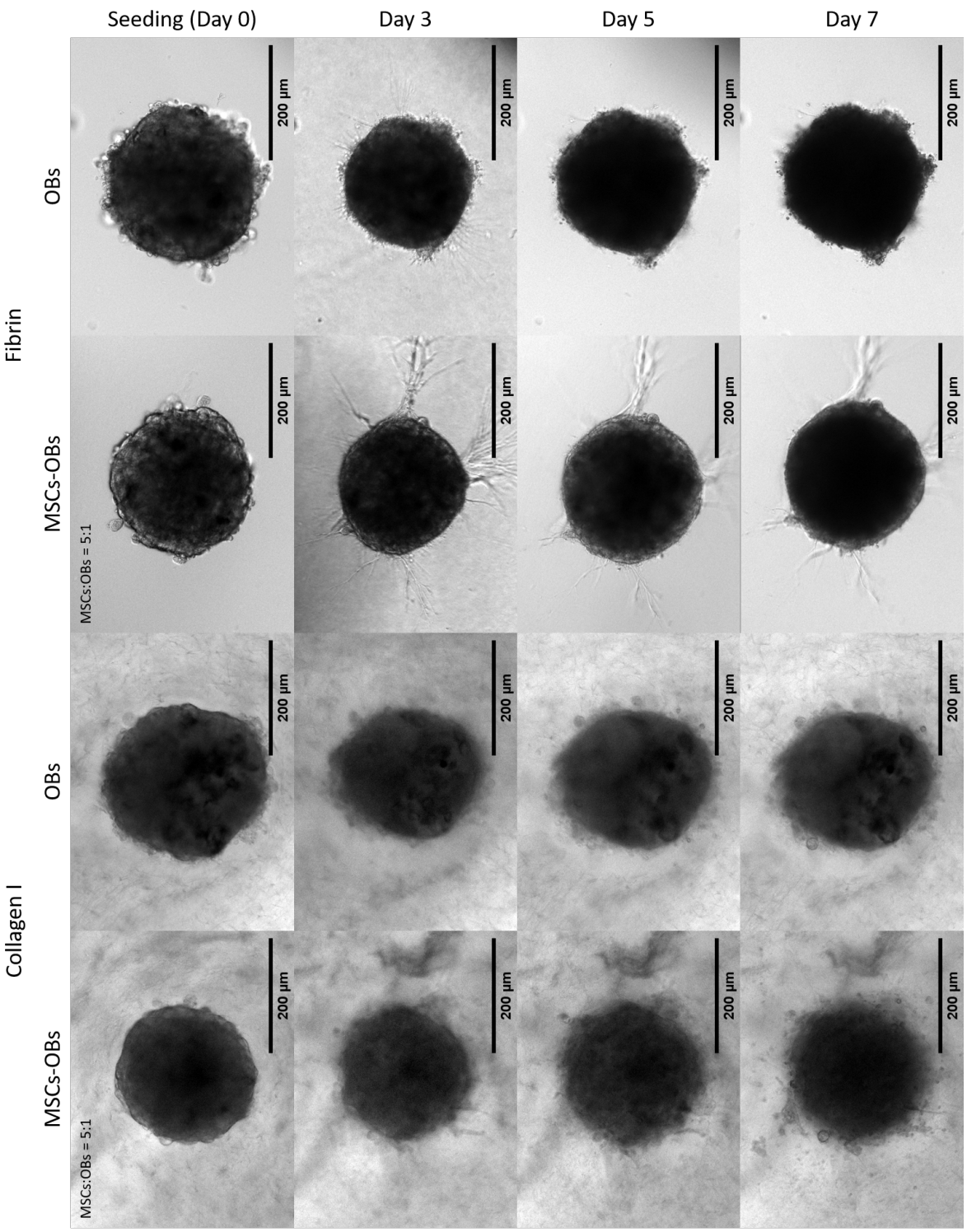

Figure 3.10: Co-culture of MSCs-OBs (5:1) and OBs spheroids in a Collagen I and Fibrin hydrogel on day 0 and after 3, 5 and 7 days.

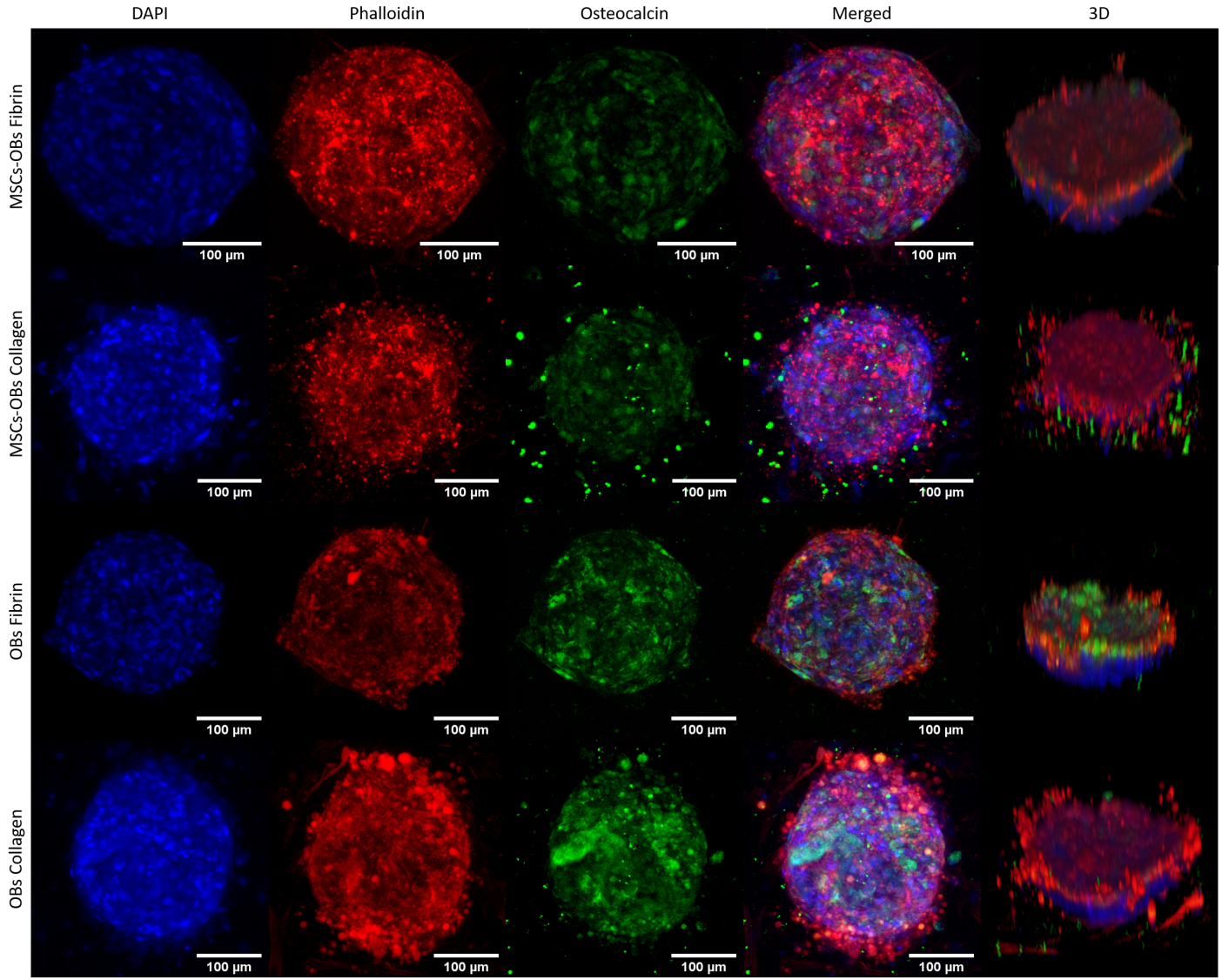

Figure 3.11: Co-culture of MSC-OB (5:1) and OB spheroids, in Collagen I and Fibrin hydrogel after 7 days stained with immunofluorescence and imaged by confocal microscopy. Blue = DAPI, Red = Phalloidin and Green = Osteocalcin. Individual images as well as merged and a 3D reconstruction.

3.3.4 BMEC spheroids

From the co-culture of MSCs with HUVECs a positive effect was visible when ECs were added to the spheroids. To form a spheroid that is even more comparable to the bone marrow tissue, BMECs were used instead of HUVECs. Co-cultures with MSCs or OBs and BMECs were performed similar to the HUVECs cultures. In Figure 3.12 MSCs-BMECs and OBs-BMECs spheroids were seeded in a Fibrin hydrogel and imaged on day 0 and after 3, 5 and 7 days.

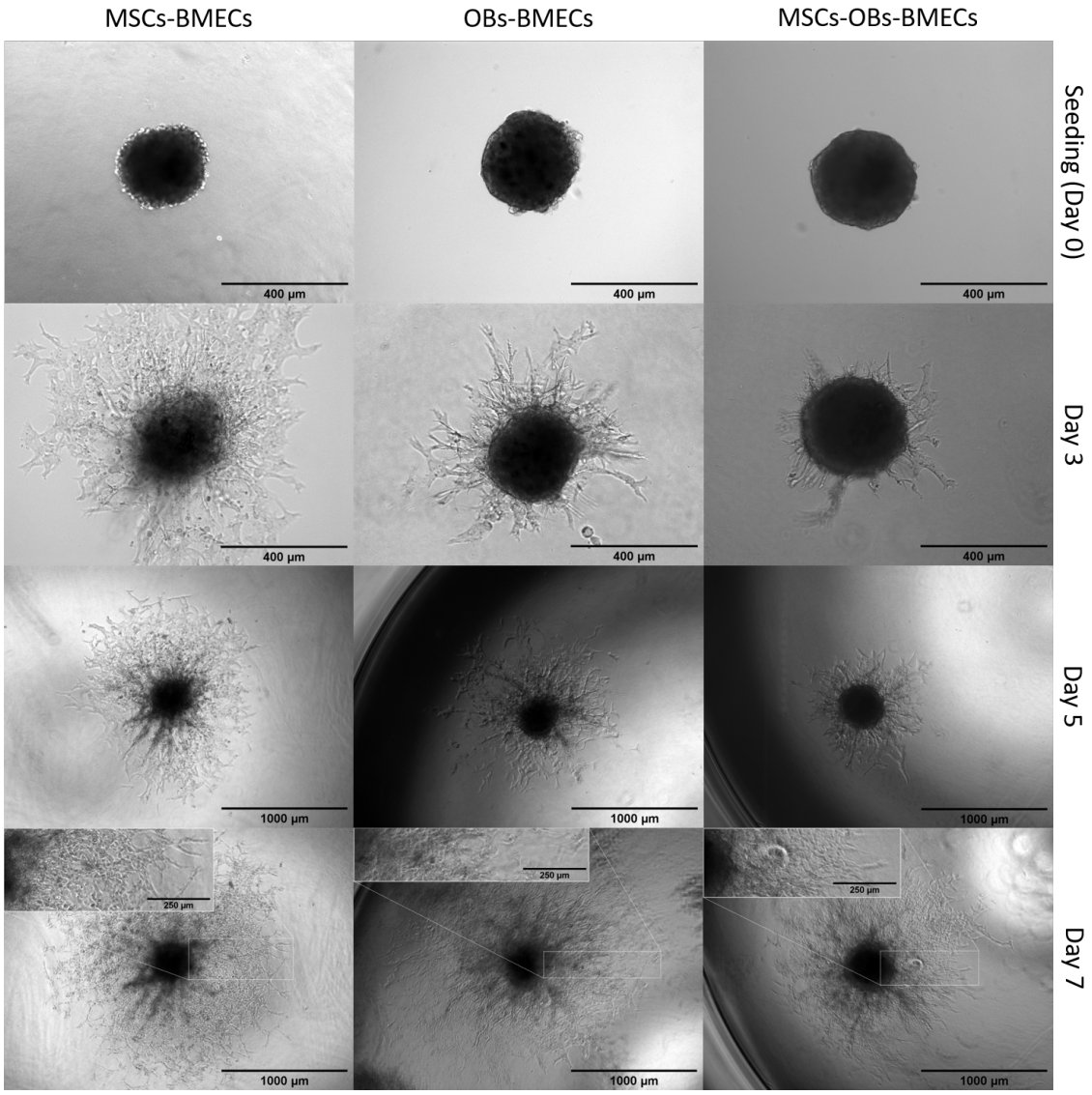

Figure 3.12: Co-culture of MSCs-BMECs (5:1), OBs-BMECs (5:1) and MSCs-OBs-BMECs (5:1:1) spheroids, in Fibrin hydrogel on day 0 and the after 3, 5 and 7 days. On day 7 a magnification of the migrated cells is presented as an inset.

The co-culture with BMECs seemed to have a very big effect on the spreading from the spheroid. Both with the MSCs and OBs large amount of cells outside the spheroid were visible, which were forming a network. This effect was also seen in the HUVEC co-culture, however the BMECs had an even stronger influence on spreading. Also, the spheroid seemed to be dispersing into this network with darker areas forming around the core of the spheroids. There was no significant difference in the co-culture with MSCs and OBs visible. Only on day 3 the OBs spheroid appeared to have a darker core compared to the MSCs and there was less spreading visible from the spheroids. On day 7 a big network was formed in all directions which is presented as an inset inf Figure 3.12.
For the formation of representative bone marrow, MSCs and OBs should be used. However, from

this co-culture the amount of spreading was minimal. So, to improve this and to eventually get better vascularization a triple-culture with MSCs, OBs and BMECs was considered. Because for the BMECs co-cultures the spreading improved the amount of spreading from the spheroids. Compared to the the MSC-OB spheroids we now see an increase in spreading, which is expected to improve the vascularization of the tissue. The increased migration from the triple-culture is similar to the amount seen in the BMECs co-cultures.
For the MSC-BMEC, OB-BMEC and MSC-OB-BMEC spheroids confocal imaging was performed after immunostaining with VE-Cadherin, Osteocalcin (Green), Phalloidin (Red) and DAPI (Blue). For the OB-BMEC and MSC-OB-BMEC Osteocalcin was used once again and for the MSC-BMEC VE-Cadherin was used, since due to the absence of OBs no Osteocalcin production was expected. In Figure 3.13 the different stainings are shown separately, together as a merge and a 3D reconstruction.
Here the spheroid itself was flattening as was seen before, and that cells are spreading form the spheroid. DAPI was present in the same places as Phalloidin staining. From the 3D reconstruction it seemed that the spheroids have flattened into some sort of crater and the cells were moving mostly sideways and downwards, but not upwards towards the nutrient source. From the Phalloidin staining the network formed by the migration cells is visible which shows that the spreading is connected to each other and vascular formation. VE-Cadherin was used to stain the endothelial cells in the culture which seem to be only in the core of the spheroid and is almost undetected. This is not expected and it could be due to a problem with the staining itself. VE-Cadherin is primarily used to stain HUVECs and could work less well on different types of ECs like BMECs.
The migration of cells is very different for the investigated conditions. For the spheroids with BMECs zoomed in fluorescent images were taken to check the morphology of the migrating cells. In Figure 3.14 four spheroid compositions were stained with DAPI and Phalloidin to visualize the morphology of the migrating cells. This includes spheroids composed of BMECs, and the other conditions are MSCs-BMECs, OBs-BMECs and MSCs-OBs-BMECs which were compared to the BMECs. For the BMEC and MSC-BMEC conditions there was an very extensive network of cells visible by actin staining. For the OB-BMEC and MSC-OB-BMEC there seemed to be a lot more gaps in the network and the cells looked more stretched.
To still image the BMECs another staining was used which should be a better marker for different types of ECs compared to VE-Cadherin, which was CD146. However, CD146 turned out be be also present on multi potent cells like MSCs, and because of this again no clear conclusion on the location of the BMECs could be drawn [79]. Along with this, a staining for RUNX2 was performed to visualize the locations where there was a higher amount of osteogenic differentiation. For this staining however there was only little amount of fluorescence present due to the limited amount of expression in the cells visible at the used magnification. To better visualize this further investigation with a higher magnification should be performed so for now this staining is not taken into consideration. One of the general limitations of the staining used is that it did not penetrate the spheroid completely. Therefore mainly cells around the border of the spheroid were stained. This could also be the reason why some of the stains were not as well visible.
The formation of a representative bone marrow requires an amount of bone mineral production which is achieved by OBs. There are however methods to increase the amount of bone production. One of these methods is the addition of HA, which is a mineral present in natural bone. Previous research has shown that the addition of HA to hydrogels increased bone formation and bone vascularization at low concentration [80, 81].

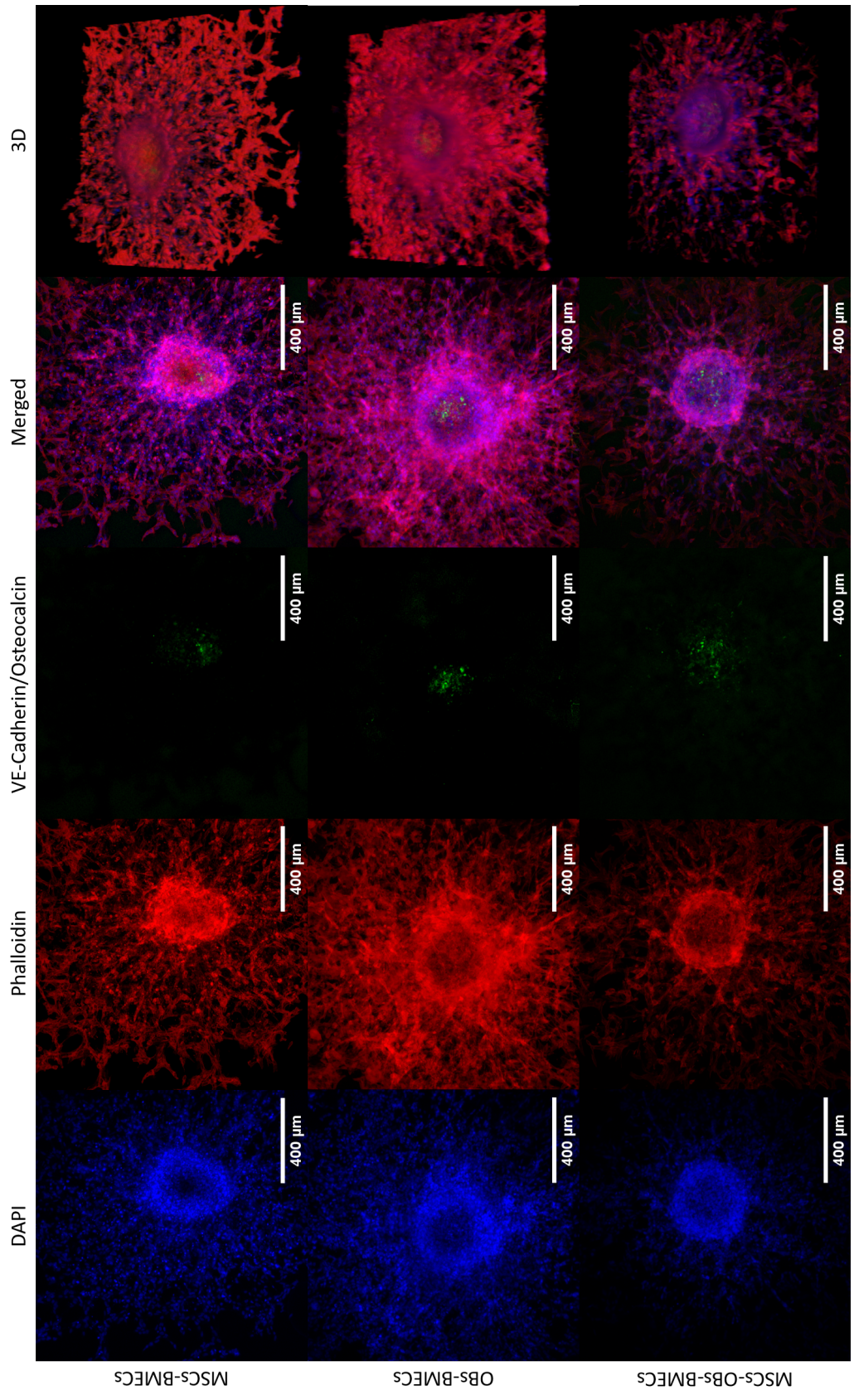

Figure 3.13: Co-culture of MSC-BMEC (5:1), OB-BMEC (5:1) and MSC-OB-BMEC (5:1:1) spheroids, in Fibrin hydrogel after 7 days stained with immunofluorescence. Blue = DAPI, Red = Phalloidin and Green = VE-Cadherin/Osteocalcin. Individual images as well as merged and a 3D reconstruction.

Figure 3.14: BMEC, MSC-BMEC (5:1), OB-BMEC (5:1) and MSC-OB-BMEC (5:1:1) spheroid imaging showing an enlargement on the migrating cells, in Fibrin hydrogel after 7 days stained with immunofluorescence. Blue = DAPI, Red = Phalloidin. Individual images as well as merged.

3.3.5 Spreading analysis

From all the spheroid cultures, cell spreading was quantified together with their size to give a better overview of the conditions.

Manual spreading analysis

In Figure 3.15 the distance from the center of the core of the spheroid to the end of the migrated cells is presented as calculated using the manual spreading analysis. A statistical analysis of the distance from the center of the core is shown in Appendix A.1.

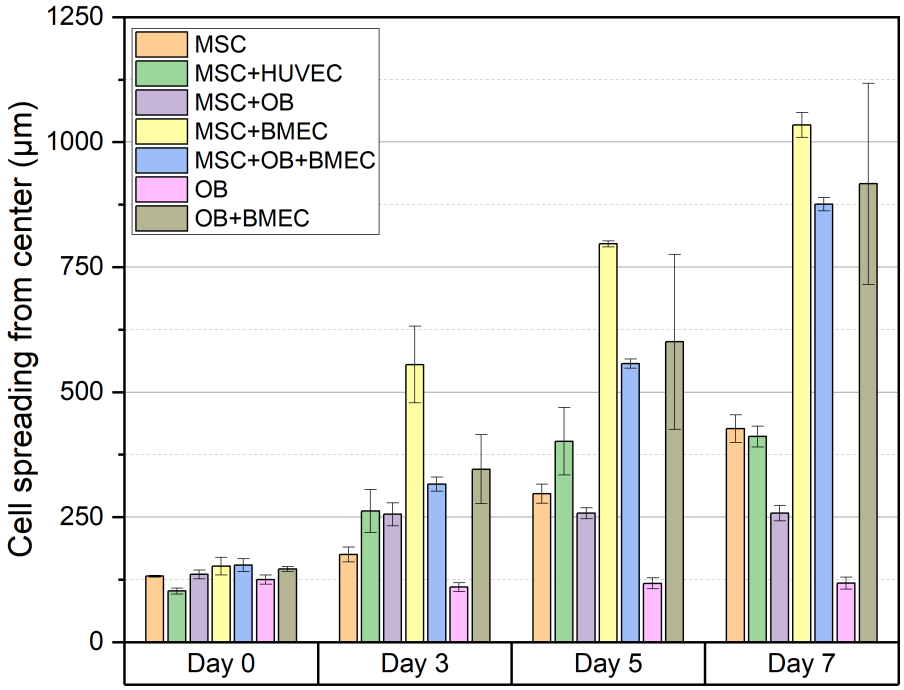

Figure 3.15: The distance from the center of the core of the spheroid towards the four furthest migrated cells on 3 different spheroids for every condition in a Fibrin hydrogel on day 0, 3, 5 and 7.

From the distance from the core on day 0 the radius of the different spheroids was determined, which was around 140 µm except for the MSC-HUVEC spheroids which were slightly smaller at around 100 µm in radius. This puts the diameter of the larger spheroids between 250 and 300 µm and the MSC-HUVEC around 200 µm. The mono-culture of the MSCs and OBs can be seen as control conditions to which co-culture models can be compared.
MSC spheroids are showing a small increase in migration at every considered time point, with a steady increase up to 427 $\pm$ 28 µm from the center of the spheroids. This was not the case for the OB spheroids, which showed no migration as already shown in Figure 3.10. To try to increase the vascularization potential HUVECs were added to MSC spheroids, which had an effect on the cell migration. After day 3 and 5 further migration was observed compared to MSC mono-culture; however at day 7 both conditions gave a similar migration distance. This shows that the HUVECs do have an initial effect on the migration, but this was not prolonged up to 7 days where no significant difference was present. When MSCs and OBs were co-cultured, it was expected that the presence of MSCs would promote cell migration compared to OBs alone. This was indeed the case and these was an increase in migration visible up to 258 $\pm$ 15 µm. The distance of migration was in between the total distance of both separate spheroid cultures, 118 $\pm$ 12 µm

and 427 $\pm$ 28 µm for OBs and MSCs respectively. Altogether an initial positive effect of on the migration of the cells was seen when HUVECs were added to MSCs and when MSCs where added to OBs. Next, the tissue-specific BMECs were used instead of HUVECs for a more bone marrow representative spheroid. The BMECs were both separately added to MSCs and OBs. After 3 days there already was a large increase in cell migration compared to the mono-cultures and the spheroids composed of MSCs-HUVECs. Cells in the MSC-BMEC spheroids migrated twice as far as the MSC-HUVEC and MSC spheroids. OB-BMEC spheroids now showed a big amount of migration compared to no migration from the OBs mono-culture, only a higher standard deviation was present in this condition.. The increase in spreading seen after 3 days continued in the next four days with a similar end point at around 1000 µm from the spheroid centre. From the images of these spheroids a different morphology was visible compared to the migration of the other spheroids, this was most likely due the difference in cells that were primarily migrating. Earlier, the MSCs seemed to be the migrating cells but now it looked like the BMECs are. This is also based on the fast proliferation of the BMEC that was seen in the 2D cultures and this can explain the huge cellular network formation. Finally, the spheroids with a triple-culture of MSCs-OBs-BMECs most optimal combination of cells for the formation of bone marrow-like tissue, gave the same large increase of migration seen for both the MSC-BMEC and OB-BMEC spheroids.
The drawback form the measurement method was that it was bias as to which migrated cells are measured and not the entire spheroid is measured.

Rectangular plot profile analysis

Apart from manually measuring the migration from the spheroids, a plot profile of the gray scale was performed. To quantify the increase in the size of the core as well as migration distance estimated. In Figure 3.16 the plot profiles of 3 different spheroids are shown. On day 0 only the spheroids is present without any cell migration, so the plot profile only showed a trough from the original spheroid. There is also a clear transition from the spheroid to the hydrogel where the trough flattens out (dashed blue line).
After 3 days there was already a significant amount of spreading into the hydrogel. Where first the trough flattened out at once there now is a slope which indicates that there was a slower transition caused by the presence of cells. Also, there were more fluctuation visible in the plots which was caused by the cellular network that is formed where lighter spots were present between the cells. The shape of the trough however remains the same up to the transition to the gel. On day 5 the curve has changed the biggest amount. Where on day 3 the trough was still in the same shape, it has now broadened which can indicate that the spheroid was growing in size. Also, the slope from the trough was broader and there are more fluctuations compared to day 3. On day 7 the changes seen in day 5 are continuing, with again a broader spectrum and more fluctuations form the cells that have migrated further into the hydrogel.
This analysis gives a similar result as was found in the manual tracing of the spreading form the spheroids. However, now also the increase of the spheroids core can be visualized better. The only drawback was that the data is less easy to interpret, because there was not always a clear transition between the core and the spreading as well and between the migrated cells and the hydrogel.
The drawback from this method was that not the entire spheroid is measured still but only a small section. Also, there was a lot of background noise from the images as well as harder interpretation of the data.

Spherical plot profile analysis

The plot profile analysis can also be performed using a spherical profile. Here the the average gray scale at a certain radius will be calculated. This gives a more complete overview of the spreading, however because a average is determined it will show less clear deviations between the spreading. In Figure 3.17 the plot profiles obtained from the MSC-BMEC, OB-BMEC and MSC-OB-BMEC cultures are shown. The dashed lines indicate the transition that is present from the migrated cells towards the hydrogel.
From this analysis it was again be seen that the projected area of the spheroid was increasing up to 7 days as well as the presence of cells outside the spheroid. The slope, that is present in all the measurements, is the transition of the spheroid core toward the hydrogel. When this slope is

gradually this indicates the presence of cells outside the spheroid core. On day 0 this peak was very sharp and flattens out quick, which indicates that there are no cells outside the core. On day 3 this slope was less sharp and also takes longer to flatten out. This indicates the transition of the the core to the cells in the hydrogel. Similar to the rectangular plot profile, there are fluctuations in the intensity that are present due to the gaps that are in between the cells. This is also visible on day 5 and 7. After day 3 a similar trend occurs where the intensity increases slower after longer culture time. This means that there are more and more cells present outside the original spheroid. Also, the darker core is increasing in radius. From the estimated transition of the migration to the hydrogel (dashed lines), the difference between the conditions was visualized better. For MSC-BMEC cells migrated furthest and OB-BMEC and MSC-OB-BMEC reach a similar distance from the center of the core.
This measurement should give the best overview of the entire spheroid because everything was measured, however both plot profile analysis suffer from background noise from the images. This was not the case for the manual method. Also, the data obtained was harder to interpret compared to the manual measurements.

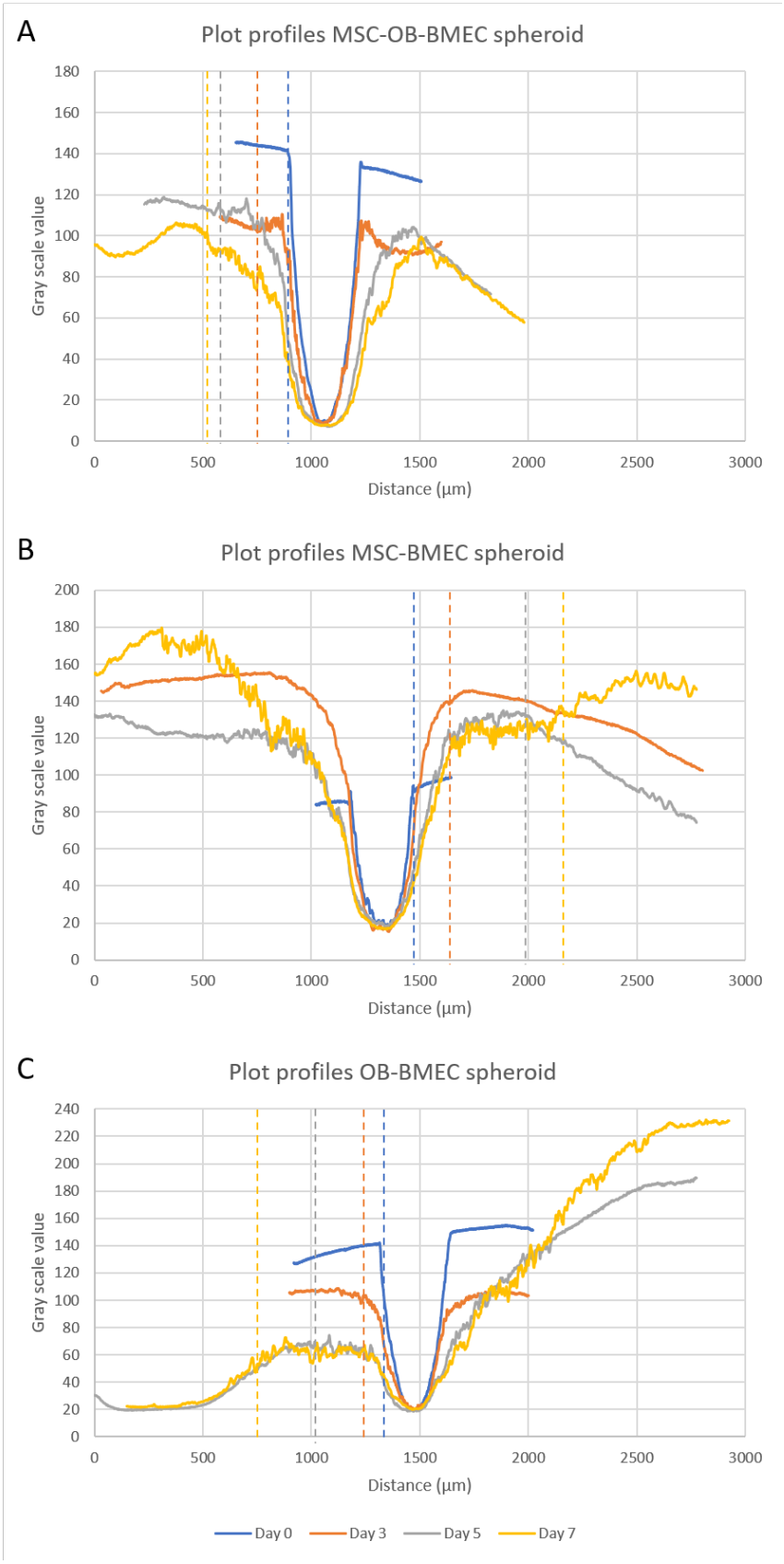

Figure 3.16: Rectangular plot profiles of MSC-BMEC, OB-BMEC and MSC-OB-BMEC spheroids on day 0 and after 3, 5 and 7 days of culture. The dashed lines indicate the estimated place where the transition from migrated cells to hydrogel occurs.

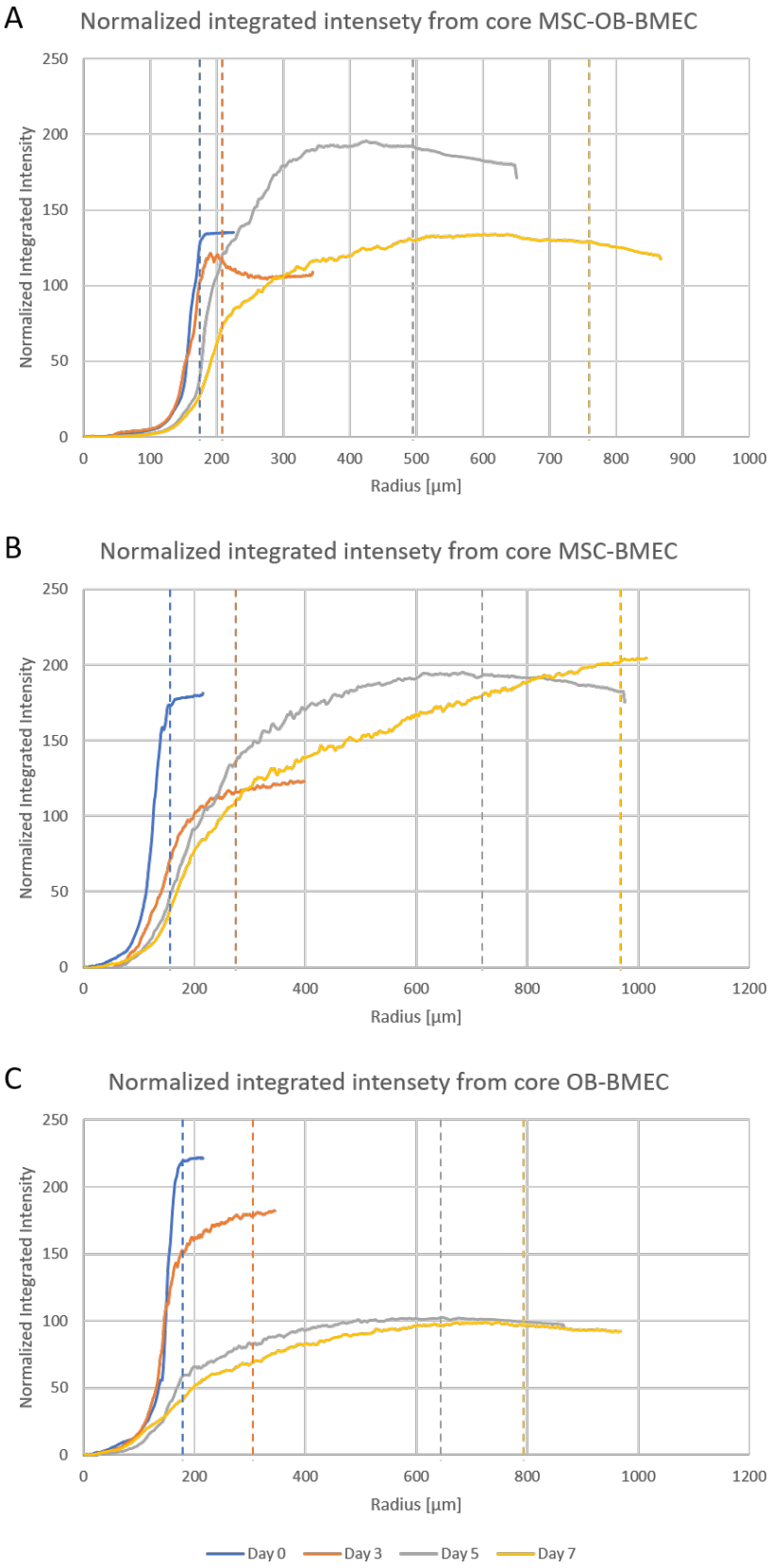

Figure 3.17: Spherical plot profiles of MSC-BMEC, OB-BMEC and MSC-OB-BMEC spheroids on day 0 and after 3, 5 and 7 days. The dashed lines indicate the estimated place where the transition from migrated cells to hydrogel occurs.

3.4 Chip fabrication

After the fabrication mould are inspected for abnormalities. Different kinds of scratches or leftover resin can be the caused by the errors during printing or in the post treatment process that have to be avoided. The printing process needed some optimization to avoid these problem but after some changes enough good mould were produced that were used for the PDMS device production. When the chip was assembled they were inspected again to ensure that the chip was bonded well to the glass slide. In Figure 3.18 a chip is shown bonded to a microscopy slide.

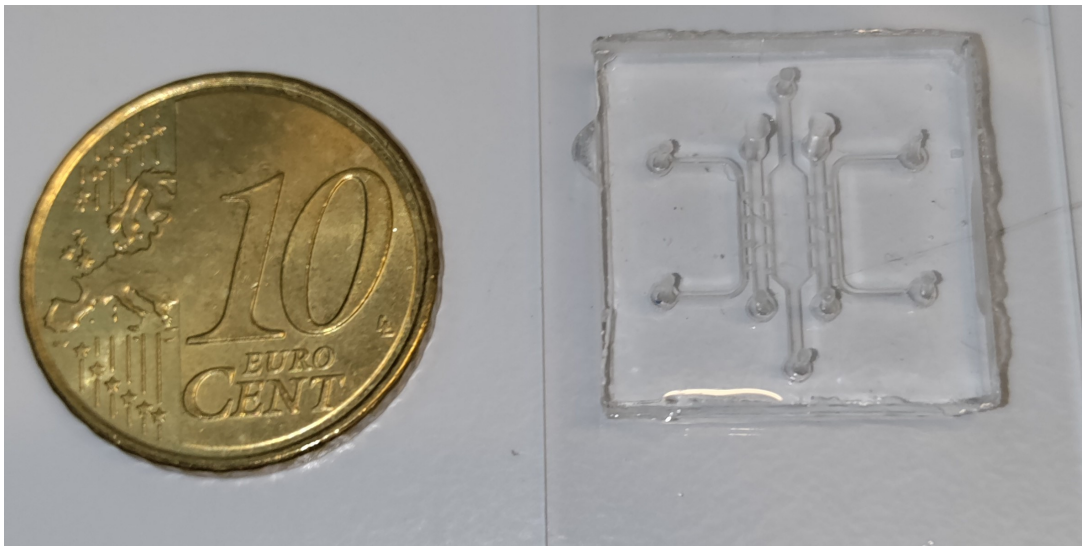

Figure 3.18: Produced PDMS chip bonded to a microscopy slide with a 10 cent coin for size reference.

3.5 On chip spheroid cultures

From the well plate cultures there were clear advantages for vascularization and imaging for the spheroid compositions as well as the hydrogel. The choice for the Fibrin hydrogel was made earlier due to the improved characteristics and the effect on the spheroids. For the on chip culture the following conditions were therefore selected: MSC-OB-BMEC, MSC-OB, OB-BMEC, MSC-BMEC and MSC. The MSCs were used as a control. The MSC-OB-BMEC triple-culture are considered as the best model for the final bone marrow formation, and other conditions were used to investigate the possible effect of the presence of different cells types.
For all conditions the same visual investigation was performed, as in Section 3.3, as well as a qPCR analysis. This qPCR analysis was compared to a well plate culture for the same spheroids. Form the on chip cultures if however appears that the spheroids are less likely to from the same spreading into the hydrogel. In some cases there was even no spreading at all, which was not found in the well plate cultures. This can be seen in Figure 3.19 for the MSC-OB, OB-BMEC and MSC conditions. In the two conditions that showed some spreading into the hydrogel, MSC-OB-BMEC and MSC-BMEC, spreading was much less compared to the well plate cultures. Because there is no difference in the spheroid composition and the hydrogel this difference must be caused by the confinement in the microfluidic chip instead of the well plate. One of the big differences is that the nutrients are now supplied from the sides of the hydrogel instead of from the top. Also, the total volume of the hydrogel is smaller.
Aside from the reduced spreading of the spheroids the gels with the cells were still extracted for qPCR analysis. Also the spheroids that did not show any migration were used to check if differences in the gene expression could explain this reduction.

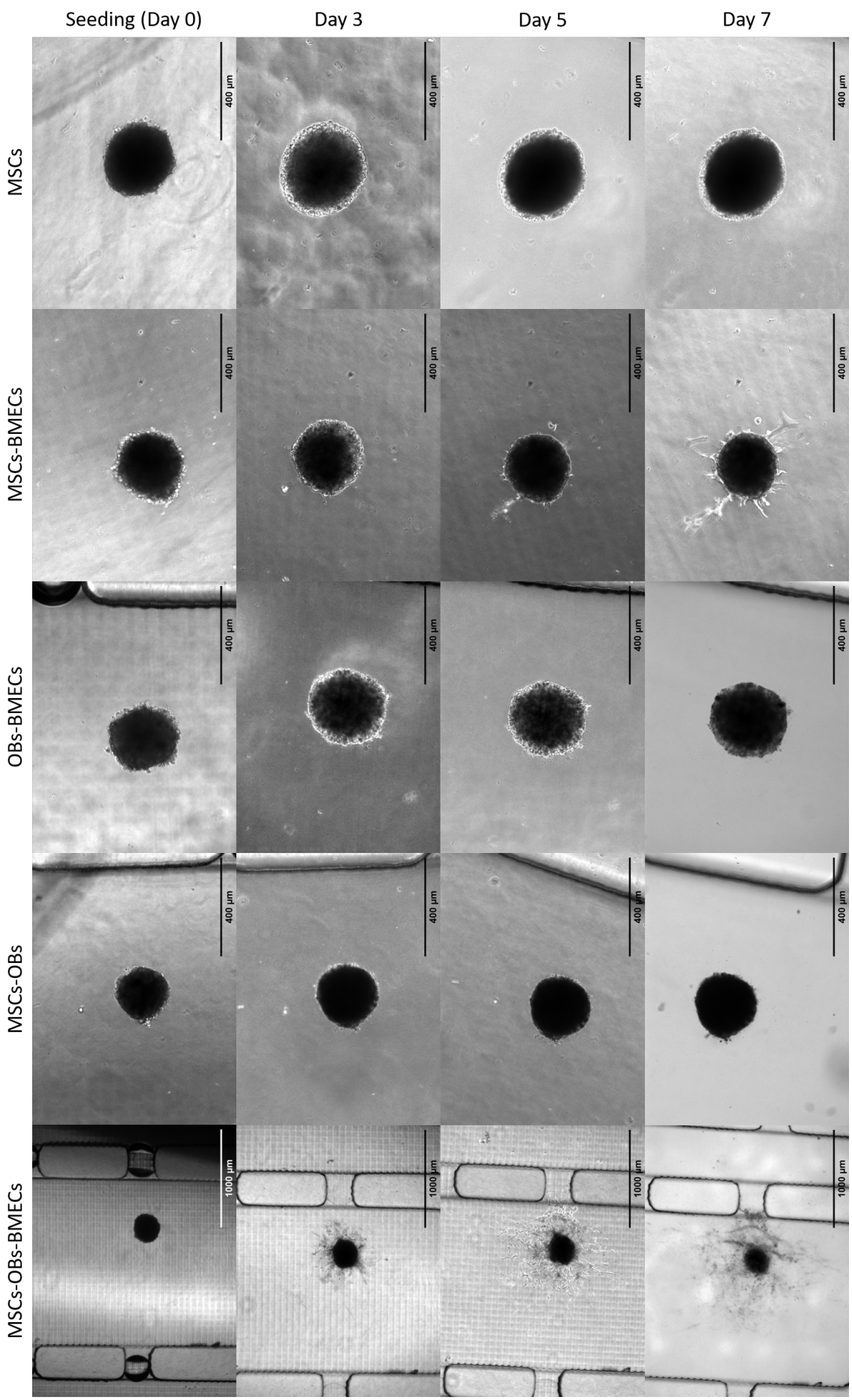

Figure 3.19: On chip culture of MSC-OB-BMEC (5:1:1), MSC-OB (5:1), OB-BMEC (5:1), MSC-BMEC (5:1) and MSC spheroids, in Fibrin hydrogel on day 0 and the after 3, 5 and 7 days of culture.

3.5.1 qPCR

For the qPCR analysis the spheroids in the hydrogels had been extracted and processed to extract the RNA. GAPDH was selected as housekeeping gene to which the other markers were normalized. Osteocalcin, Osterix, Osteonectin, Osteopontin, RUNX2, and Collagen I were selected as osteogenic differentiation and bone formation markers [82]. Nestin is a bone development and HSC maintenance marker essential for the long-term sustainment of HSCs [83]. ICAM-1 was selected as a vacularization marker which is expressed during angiogenesis as well as a marker for HSC niche adhesion. Fibronectin is an important part of the ECM in the bone marrow and known to mediate HSC homing [84]. Collagen II and Collagen X were used as markers that could indicate the differentiation into cartilage tissue instead of bone.
From the different conditions the RNA was quantified but not for all the samples there was enough RNA present to produce sufficient amounts of cDNA for qPCR. Therefore, some of the markers have been removed for these conditions. Primarily the conditions that were cultured in the wells plate showed a low RNA content. This can be caused by the higher hydrogel to cell ratio that was present in the well plate cultures which can interfere with the RNA extraction. These well plate conditions would be considered as a control but because the qPRC could not be performed for these conditions only the ΔCt values could be calculated and not the relative fold gene expression level. So, the obtained ΔCt values can still be compared to the different conditions. Also, there were some discrepancies in the amplification of the genes within the same conditions. Therefore, the experiment needs to be repeated to add the missing conditions and primers. Because all the data is relative to the housekeeping gene this can than still be compared. In Figure 3.20 the obtained ΔCt values for the different conditions and primers are shown.

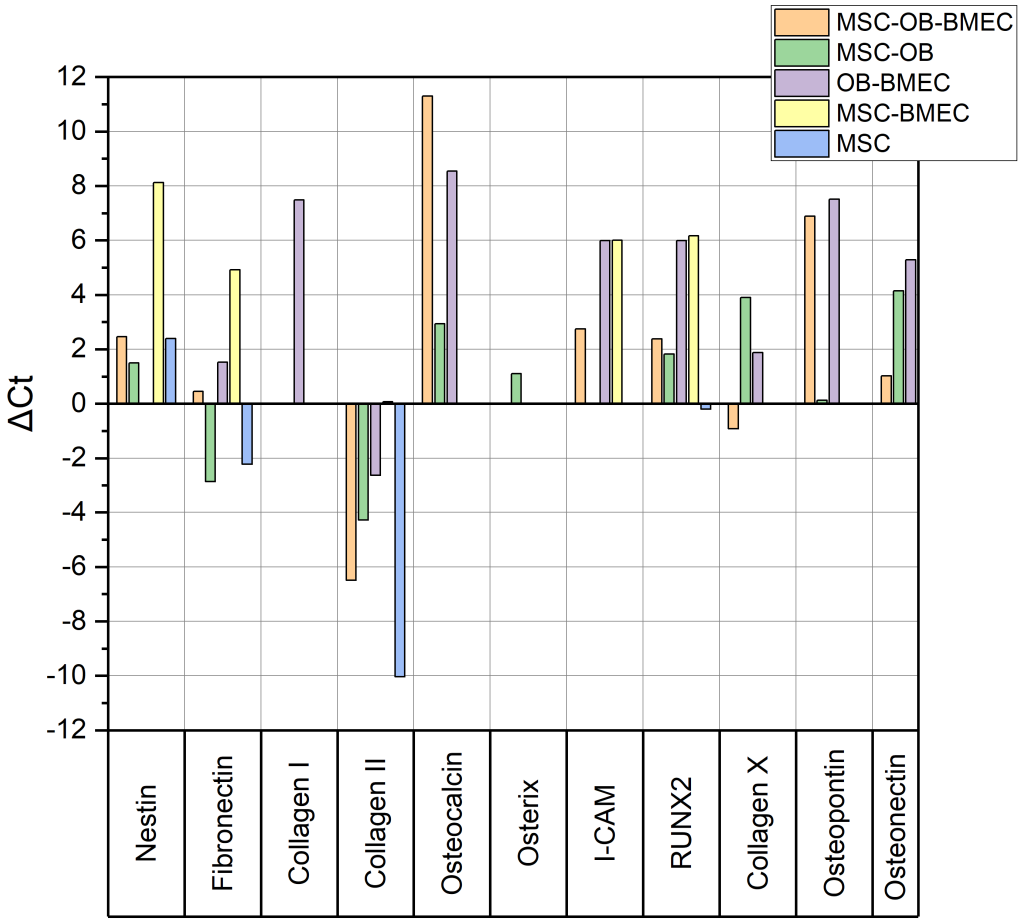

Figure 3.20: ΔCt values for the different conditions and primers.

Nestin is present in all spheroids except in the OBs-BMECs with could be due to the lack of MSCs

which produce this for the HSCs maintenance. Fibronectin is also present in all spheroids, but there is no clear distribution in the protein expression. Collagen I only shows a high expression in the OBs-BMECs condition, from this very little can be deduced. Collagen II however shows a relative low expressions compared to the housekeeping gene, only for the MSCs-BMECs condition there is a small positive value. Osteocalcin, Osteopontin and Osteonectin are only present in spheroids with OBs. This is to be expected because these proteins are only produced by osteogenic cells. Osterix however only shows a activity in the MSCs-OBs condition. I-CAM present only in spheroids with BMECs and this shows that there is only angiogenesis in the spheroids with ECs. RUNX2 is present in all spheroids but is more expressed in the co-cultures. This shows that there is osteogenic differentiation also in the cultures without OBs. Collagen X also shows only activity in the OBs conditions with could indicate some chondrogenesis in the tissue as well as the Collagen II expression.

3.6 Endothelial lumen

Due to a drawback in the chip production the on-chip cultures were shifted into a well plate culture early on. Because of this, the formation of the tissue specific endothelial lumen was not possible at an early stage and focus shifted more towards the investigation of the migration from the spheroids. Some first experiments with the formation of the lumen with BMECs were performed that are shown in Figure 3.21. Here you can seen the lumen channel with a Collagen I lumen and filled with BMECs. The red lines mark the border between the cells and the hydrogel. Further investigation of the lumen formation alone and in combination with the bone marrow tissue still needs to be performed.

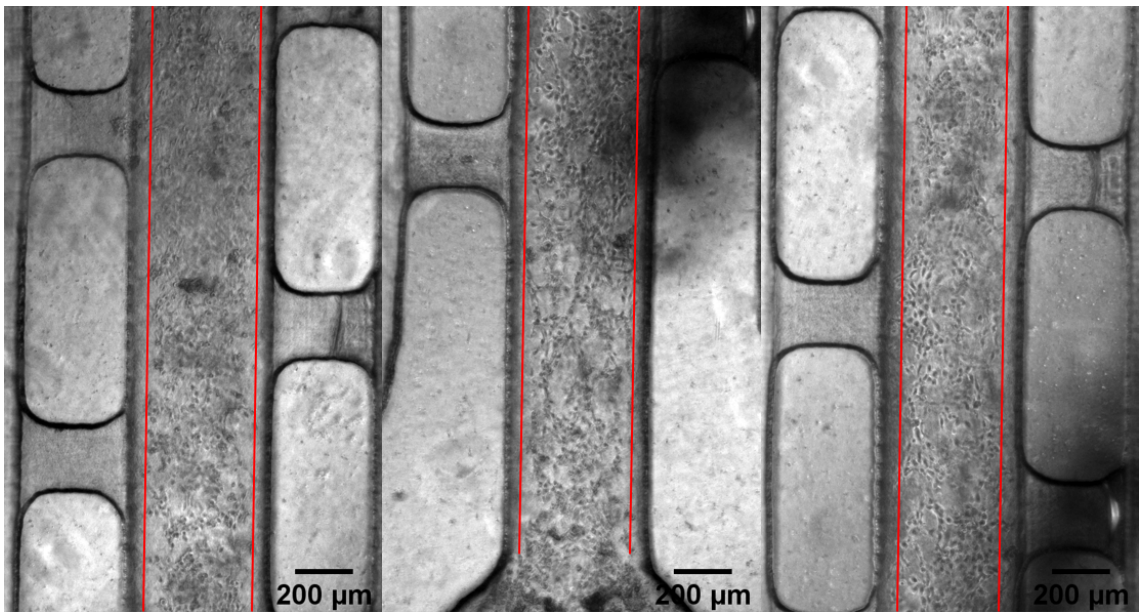

Figure 3.21: Vascular lumen lined with BMECs. The red lines indicate the area where the lumen transitions into the hydrogel, here are no cells present.

4 CONCLUSION

In this report the early development of a bone marrow like tissue on chip has been investigated. The effects of MSCs, OBs and ECs on the tissue formation, and their combinations was the primary focus of this study.
First, the formation of spheroids with different compositions was performed in the microwell arrays and the absence of a necrotic core determined to ensure the adequate delivery of nutrients for which the $2 * 10^6$ cells/microwell array proved sufficient. Also, the morphological effects of the different compositions were investigated as well as the optimum of culture time of 2 days in the mirowell array.
Next, the formed spheroids were seeded in two hydrogels. From the early hydrogel cultures it was clear that the Fibrin hydrogel showed improved cellular organization shown by cells spreading from the spheroid into the hydrogel. It was also shown in literature that a Fibrin hydrogel has its advantages compared to Collagen I hydrogels when vascular organization is a goal [76].
During the experimental testing of the best hydrogel, also the best composition of spheroids for most representative bone marrow tissue is investigated. In the bone marrow a combination of MSCs and other bone cells are present so this was included by differentiating MSCs to OBs. These two cell types are then used in combination with HUVECs and BMECs which improved the the vascular migration into the hydrogel. From these cultures a optimal spheroid composition with MSCs, OBs and BMECs is found.
Next, the best conditions obtained from the hydrogel and spheroids optimization cultures in the wells plate, are used in the chip as well. However, the consistency of the spheroids cultured in the chips was not similar to the wells plates. This has to be investigated further to determine why, it is possible that because of the confinement in the chip the cells are less likely to migrate into the hydrogel. When combining the spheroid in the chip with the vascular lumen this could also be resolved due to the presence of cells in the vascular channel.

5 FUTURE PERSPECTIVES

In this study, the first steps have been performed towards the development of a bone marrow like tissue using different combinations of spheroid composition and hydrogels. From the investigated conditions, the most suitable has been selected to be characterized more complete in order to confirm the representativeness of the formed tissue.
The primary focus has been to form the tissue in the microfluidic chips, however this has been mostly performed using wells plates instead. When the spheroids are cultured in the chips the results are not always similar so this still needs to be optimized. When this is completed a more extensive analysis of the tissue formation can be performed using immunofluorescence and qPCR. For For the qPCR, control measurements need to be performed, this can be done by analyzing the spheroids before they are introduced into the hydrogel. These values can then be used to compare and quantify the gene expression better.
Aside from the tissue formation, the vascular lumen also needs to be included. There have already been some trials with the BMEC lumen formation that have been performed in a separate part of the CHIP-ME project for now. The vessel formation with the BMECs do show promising results and can be combined in the microfluidic chip when the bone marrow tissue formation is consistent. When the lumen has been included, the chip can be connected to the developed circulation setup and the extravasation of CTCs into the tissue can be investigated.
Because OBs are included into the tissue there could also be some differentiation into osteocytes, as mentioned before. It would also be interesting to include staining or qPCR primer that are expressed when OBs are differentiating further [37]. The addition of HA to the hydrogel would also have an influence of the amount of bone formation, and this still needs to be investigated, which could improve a more bone like tissue formation [80, 81]. Also, the MSCs are known to differentiate into pericyte like cells that are able maintain the formed vascularization so this can also be looked into further [85].
Before the choice for the hydrogel was made there where vesicles visible in the cultures with a Collagen I hydrogel. The nature and origin of these vesicles still needs to be investigated. They could be apoptotic bodies or EVs and and for these two possibilities immunostaining can be performed with ApoTracker and CD9 or CD81.

REFERENCES

[1] H. Sung, J. Ferlay, R. L. Siegel et al., Global cancer statistics 2020: GLOBOCAN estimates of incidence and mortality worldwide for 36 cancers in 185 countries, CA: A Cancer Journal for Clinicians (2021) caac.21660doi:10.3322/caac.21660.

[2] J. Budczies, M. von Winterfeld, F. Klauschen et al., The landscape of metastatic progression patterns across major human cancers, Oncotarget 6 (1) (2015) 570–583. doi:10.18632/oncotarget.2677.

[3] G. P. Gupta J. Massagué, Cancer Metastasis: Building a Framework, Cell 127 (4) (2006) 679–695. doi:10.1016/j.cell.2006.11.001.

[4] D. Caballero, S. Kaushik, V. Correlo et al., Organ-on-chip models of cancer metastasis for future personalized medicine: From chip to the patient, Biomaterials 149 (2017) 98–115. doi:10.1016/j.biomaterials.2017.10.005.

[5] F. Macedo, K. Ladeira, F. Pinho et al., Bone metastases: an overview, Oncology Reviews 11:321. doi:10.4081/oncol.2017.321.

[6] M. Riihimäki, H. Thomsen, K. Sundquist et al., Clinical landscape of cancer metastases, Cancer Medicine 7 (11) (2018) 5534–5542. doi:10.1002/cam4.1697.

[7] J. Fares, M. Y. Fares, H. H. Khachfe et al., Molecular principles of metastasis: a hallmark of cancer revisited, Signal Transduction and Targeted Therapy 5 (1) (2020) 28. doi:10.1038/s41392-020-0134-x.

[8] J. Massagué A. C. Obenauf, Metastatic colonization by circulating tumour cells, Nature 529 (7586) (2016) 298–306. doi:10.1038/nature17038.

[9] K. N. Weilbaecher, T. A. Guise L. K. McCauley, Cancer to bone: a fatal attraction, Nature Reviews Cancer 11 (6) (2011) 411–425. doi:10.1038/nrc3055.

[10] A. F. Chambers, A. C. Groom I. C. MacDonald, Dissemination and growth of cancer cells in metastatic sites, Nature Reviews Cancer 2 (8) (2002) 563–572. doi:10.1038/nrc865.

[11] Y. A. Fouad C. Aanei, Revisiting the hallmarks of cancer, American journal of cancer research 7 (5) (2017) 1016–1036.

[12] D. Ribatti, G. Mangialardi A. Vacca, Stephen Paget and the 'seed and soil' theory of metastatic dissemination, Clinical and Experimental Medicine 6 (4) (2006) 145–149. doi:10.1007/s10238-006-0117-4.

[13] S. Paget, THE DISTRIBUTION OF SECONDARY GROWTHS IN CANCER OF THE BREAST., The Lancet 133 (3421) (1889) 571–573. doi:10.1016/S0140-6736(00)49915-0.

[14] T. Tsuji, S. Ibaragi G.-f. Hu, Epithelial-Mesenchymal Transition and Cell Cooperativity in Metastasis, Cancer Research 69 (18) (2009) 7135–7139. doi:10.1158/0008-5472.CAN-09-1618.

[15] M. Bockhorn, R. K. Jain L. L. Munn, Active versus passive mechanisms in metastasis: do cancer cells crawl into vessels, or are they pushed?, The Lancet Oncology 8 (5) (2007) 444–448. doi:10.1016/S1470-2045(07)70140-7.

[16] I. K. Zervantonakis, S. K. Hughes-Alford, J. L. Charest et al., Three-dimensional microfluidic model for tumor cell intravasation and endothelial barrier function, Proceedings of the National Academy of Sciences 109 (34) (2012) 13515–13520. doi:10.1073/pnas.1210182109.

[17] C. M. Denais, R. M. Gilbert, P. Isermann et al., Nuclear envelope rupture and repair during cancer cell migration, Science 352 (6283) (2016) 353–358. doi:10.1126/science.aad7297.

[18] D. Gao, E. W. Thompson V. Mittal, EMT process in bone metastasis, in: Bone Cancer, Elsevier, 2015, pp. 451–459. doi:10.1016/B978-0-12-416721-6.00038-8.

[19] M. Yu, A. Bardia, B. S. Wittner et al., Circulating Breast Tumor Cells Exhibit Dynamic Changes in Epithelial and Mesenchymal Composition, Science 339 (6119) (2013) 580–584. doi:10.1126/science.1228522.

[20] K. Pantel M. R. Speicher, The biology of circulating tumor cells, Oncogene 35 (10) (2016) 1216–1224. doi:10.1038/onc.2015.192.

[21] N. Aceto, A. Bardia, D. T. Miyamoto et al., Circulating Tumor Cell Clusters Are Oligoclonal Precursors of Breast Cancer Metastasis, Cell 158 (5) (2014) 1110–1122. doi:10.1016/j.cell.2014.07.013.

[22] J. A. Joyce J. W. Pollard, Microenvironmental regulation of metastasis, Nature Reviews Cancer 9 (4) (2009) 239–252. doi:10.1038/nrc2618.

[23] S. Valastyan R. A. Weinberg, Tumor Metastasis: Molecular Insights and Evolving Paradigms, Cell 147 (2) (2011) 275–292. doi:10.1016/j.cell.2011.09.024.

[24] D. Stegner, S. Dütting B. Nieswandt, Mechanistic explanation for platelet contribution to cancer metastasis, Thrombosis Research 133 (2014) S149–S157. doi:10.1016/S0049-3848(14)50025-4.

[25] K. Stoletov, H. Kato, E. Zardouzian et al., Visualizing extravasation dynamics of metastatic tumor cells, Journal of Cell Science 123 (13) (2010) 2332–2341. doi:10.1242/jcs.069443.

[26] F. L. Miles, F. L. Pruitt, K. L. van Golen et al., Stepping out of the flow: capillary extravasation in cancer metastasis, Clinical & Experimental Metastasis 25 (4) (2008) 305–324. doi:10.1007/s10585-007-9098-2.

[27] N. Reymond, B. B. D'Água A. J. Ridley, Crossing the endothelial barrier during metastasis, Nature Reviews Cancer 13 (12) (2013) 858–870. doi:10.1038/nrc3628.

[28] N. Nishida, H. Yano, T. Nishida et al., Angiogenesis in cancer, Vascular Health and Risk Management 2 (3) (2006) 213–219. doi:10.2147/vhrm.2006.2.3.213.

[29] B. J. Bain, D. M. Clark B. S. Wilkins, Bone Marrow Pathology, Wiley-Blackwell, Oxford, UK, 2009. doi:10.1002/9781444309782.

[30] U. A. Gurkan O. Akkus, The Mechanical Environment of Bone Marrow: A Review, Annals of Biomedical Engineering 36 (12) (2008) 1978–1991. doi:10.1007/s10439-008-9577-x.

[31] G. J. Cabrita, B. S. Ferreira, C. L. da Silva et al., Hematopoietic stem cells: from the bone to the bioreactor, Trends in Biotechnology 21 (5) (2003) 233–240. doi:10.1016/S0167-7799(03)00076-3.

[32] A. I. Caplan, Mesenchymal Stem Cells: Time to Change the Name!, STEM CELLS Translational Medicine 6 (6) (2017) 1445–1451. doi:10.1002/sctm.17-0051.

[33] M. Chavez-MacGregor, Angiogenesis in the Bone Marrow of Patients with Breast Cancer, Clinical Cancer Research 11 (15) (2005) 5396–5400. doi:10.1158/1078-0432.CCR-04-2420.

[34] G. D. Roodman, Pathophysiology of Bone Metastases, in: Bone Metastases. Cancer Metastasis – Biology and Treatment, 12th Edition, Springer, 2009, pp. 31–50. doi:10.1007/978-1-4020-9819-2_2.

[35] K. M. Bussard, C. V. Gay A. M. Mastro, The bone microenvironment in metastasis; what is special about bone?, Cancer and Metastasis Reviews 27 (1) (2008) 41–55. doi:10.1007/s10555-007-9109-4.

[36] C. Vrahnas N. A. Sims, Basic Aspects of Osteoblast Function, in: Osteoporosis, Humana Press, 2020, pp. 1–16. doi:10.1007/978-3-319-69287-6_1.

[37] R. Florencio-Silva, G. R. d. S. Sasso, E. Sasso-Cerri et al., Biology of Bone Tissue: Structure, Function, and Factors That Influence Bone Cells, BioMed Research International 2015 (2015) 1–17. doi:10.1155/2015/421746.

[38] E. N. Marieb K. Hoehn, Human Anatomy and Physiology 9th Edition, Pearson, 2013.

[39] J. Delgado-Calle T. Bellido, Basic Aspects of Osteocyte Function, in: Osteoporosis, Humana Press, 2020, pp. 43–69. doi:10.1007/978-3-319-69287-6_3.

[40] N. Alesi, J. F. Charles M. C. Nakamura, Basic Aspects of Osteoclast Differentiation and Function, in: Osteoporosis, Humana Press, 2020, pp. 17–41. doi:10.1007/978-3-319-69287-6_2.

[41] M. A. Lichtman, W. J. Williams, T. J. Kipps et al., Williams Hematology, 8th Edition, McGraw-Hill, 2010.

[42] M. Capulli, R. Paone N. Rucci, Osteoblast and osteocyte: Games without frontiers, Archives of Biochemistry and Biophysics 561 (2014) 3–12. doi:10.1016/j.abb.2014.05.003.

[43] J. Scheinpflug, M. Pfeiffenberger, A. Damerau et al., Journey into Bone Models: A Review, Genes 9 (5) (2018) 247. doi:10.3390/genes9050247.

[44] G. Bresciani, L. J. Hofland, F. Dogan et al., Evaluation of Spheroid 3D Culture Methods to Study a Pancreatic Neuroendocrine Neoplasm Cell Line, Frontiers in Endocrinology 10. doi:10.3389/fendo.2019.00682.

[45] Z. Cesarz K. Tamama, Spheroid Culture of Mesenchymal Stem Cells, Stem Cells International 2016 (2016) 1–11. doi:10.1155/2016/9176357.

[46] G. Turnbull, J. Clarke, F. Picard et al., 3D bioactive composite scaffolds for bone tissue engineering, Bioactive Materials 3 (3) (2018) 278–314. doi:10.1016/j.bioactmat.2017.10.001.

[47] V. S. Kattimani, S. Kondaka K. P. Lingamaneni, Hydroxyapatite–-Past, Present, and Future in Bone Regeneration, Bone and Tissue Regeneration Insights 7 (2016) BTRI.S36138. doi:10.4137/BTRI.S36138.

[48] U. Blache M. Ehrbar, Inspired by Nature: Hydrogels as Versatile Tools for Vascular Engineering, Advances in Wound Care 7 (7) (2018) 232–246. doi:10.1089/wound.2017.0760.

[49] M. E. Katt, A. L. Placone, A. D. Wong et al., In Vitro Tumor Models: Advantages, Disadvantages, Variables, and Selecting the Right Platform, Frontiers in Bioengineering and Biotechnology 4. doi:10.3389/fbioe.2016.00012.

[50] A. Mansoorifar, R. Gordon, R. C. Bergan et al., Bone-on-a-Chip: Microfluidic Technologies and Microphysiologic Models of Bone Tissue, Advanced Functional Materials (2020) 2006796doi:10.1002/adfm.202006796.

[51] P. McGonigle B. Ruggeri, Animal models of human disease: Challenges in enabling translation, Biochemical Pharmacology 87 (1) (2014) 162–171. doi:10.1016/j.bcp.2013.08.006.

[52] D. Huh, G. A. Hamilton D. E. Ingber, From 3D cell culture to organs-on-chips, Trends in Cell Biology 21 (12) (2011) 745–754. doi:10.1016/j.tcb.2011.09.005.

[53] L. A. Low, C. Mummery, B. R. Berridge et al., Organs-on-chips: into the next decade, Nature Reviews Drug Discoverydoi:10.1038/s41573-020-0079-3.

[54] D. Qin, Y. Xia G. M. Whitesides, Soft lithography for micro- and nanoscale patterning, Nature Protocols 5 (3) (2010) 491–502. doi:10.1038/nprot.2009.234.

[55] A. Secord S. Siamakpour-Reihani, Angiogenesis, in: Translational Advances in Gynecologic Cancers, Elsevier, 2017, pp. 79–109. doi:10.1016/B978-0-12-803741-6.00005-7.

[56] P. Carmeliet R. K. Jain, Angiogenesis in cancer and other diseases, Nature 407 (6801) (2000) 249–257. doi:10.1038/35025220.

[57] A. C. Newman, M. N. Nakatsu, W. Chou et al., The requirement for fibroblasts in angiogenesis: fibroblast-derived matrix proteins are essential for endothelial cell lumen formation, Molecular Biology of the Cell 22 (20) (2011) 3791–3800. doi:10.1091/mbc.e11-05-0393.

[58] L. L. Bischel, E. W. Young, B. R. Mader et al., Tubeless microfluidic angiogenesis assay with three-dimensional endothelial-lined microvessels, Biomaterials 34 (5) (2013) 1471–1477. doi:10.1016/j.biomaterials.2012.11.005.

[59] A. Sobrino, D. T. T. Phan, R. Datta et al., 3D microtumors in vitro supported by perfused vascular networks, Scientific Reports 6 (1) (2016) 31589. doi:10.1038/srep31589.

[60] S. Kim, H. Lee, M. Chung et al., Engineering of functional, perfusable 3D microvascular networks on a chip, Lab on a Chip 13 (8) (2013) 1489. doi:10.1039/c3lc41320a.

[61] Y. Nashimoto, T. Hayashi, I. Kunita et al., Integrating perfusable vascular networks with a three-dimensional tissue in a microfluidic device, Integrative Biology 9 (6) (2017) 506–518. doi:10.1039/C7IB00024C.

[62] L. L. Bischel, S.-H. Lee D. J. Beebe, A Practical Method for Patterning Lumens through ECM Hydrogels via Viscous Finger Patterning, Journal of Laboratory Automation 17 (2) (2012) 96–103. doi:10.1177/2211068211426694.

[63] D. B. Chou, V. Frismantas, Y. Milton et al., On-chip recapitulation of clinical bone marrow toxicities and patient-specific pathophysiology, Nature Biomedical Engineering 4 (4) (2020) 394–406. doi:10.1038/s41551-019-0495-z.

[64] J. S. Jeon, I. K. Zervantonakis, S. Chung et al., In Vitro Model of Tumor Cell Extravasation, PLoS ONE 8 (2) (2013) e56910. doi:10.1371/journal.pone.0056910.

[65] D. Kefallinou, M. Grigoriou, D. T. Boumpas et al., Fabrication of a 3D microfluidic cell culture device for bone marrow-on-a-chip, Micro and Nano Engineering 9 (2020) 100075. doi:10.1016/j.mne.2020.100075.

[66] S. Bersini, J. S. Jeon, G. Dubini et al., A microfluidic 3D in vitro model for specificity of breast cancer metastasis to bone, Biomaterials 35 (8) (2014) 2454–2461. doi:10.1016/j.biomaterials.2013.11.050.

[67] J. S. Jeon, S. Bersini, M. Gilardi et al., Human 3D vascularized organotypic microfluidic assays to study breast cancer cell extravasation, Proceedings of the National Academy of Sciences 112 (1) (2015) 214–219. doi:10.1073/pnas.1417115112.

[68] M. Absher, Hemocytometer Counting, in: Tissue Culture, Elsevier, 1973, pp. 395–397. doi:10.1016/B978-0-12-427150-0.50098-X.

[69] A. Sridhar, H. L. de Boer, A. van den Berg et al., Microstamped Petri Dishes for Scanning Electrochemical Microscopy Analysis of Arrays of Microtissues, PLoS ONE 9 (4) (2014) e93618. doi:10.1371/journal.pone.0093618.

[70] D. L. Priwitaningrum, J.-B. G. Blondé, A. Sridhar et al., Tumor stroma-containing 3D spheroid arrays: A tool to study nanoparticle penetration, Journal of Controlled Release 244 (2016) 257–268. doi:10.1016/j.jconrel.2016.09.004.

[71] Y. J. Chuah, Y. T. Koh, K. Lim et al., Simple surface engineering of polydimethylsiloxane with polydopamine for stabilized mesenchymal stem cell adhesion and multipotency, Scientific Reports 5 (1) (2016) 18162. doi:10.1038/srep18162.

[72] H. PUCHTLER, S. N. MELOAN M. S. TERRY, On the history and mechanism of Alizarin and Alizarin red S stains for Calcium, Journal of Histochemistry & Cytochemistry 17 (2) (1969) 110–124. doi:10.1177/17.2.110.

[73] E. Redondo-Castro, C. Cunningham, S. Cain et al., Generation of Human Mesenchymal Stem Cell 3D Spheroids Using Low-binding Plates, BIO-PROTOCOL 8 (16). doi:10.21769/BioProtoc.2968.

[74] W. Souza, S. G. Piperni, P. Laviola et al., The two faces of titanium dioxide nanoparticles bio-camouflage in 3D bone spheroids, Scientific Reports 9 (1) (2019) 9309. doi:10.1038/s41598-019-45797-6.

[75] Y. K. Park, T.-Y. Tu, S. H. Lim et al., In Vitro Microvessel Growth and Remodeling within a Three-Dimensional Microfluidic Environment, Cellular and Molecular Bioengineering 7 (1) (2014) 15–25. doi:10.1007/s12195-013-0315-6.

[76] R. R. Rao, A. W. Peterson, J. Ceccarelli et al., Matrix composition regulates three-dimensional network formation by endothelial cells and mesenchymal stem cells in collagen/fibrin materials, Angiogenesis 15 (2) (2012) 253–264. doi:10.1007/s10456-012-9257-1.

[77] D. N. Heo, M. Hospodiuk I. T. Ozbolat, Synergistic interplay between human MSCs and HUVECs in 3D spheroids laden in collagen/fibrin hydrogels for bone tissue engineering, Acta Biomaterialia 95 (2019) 348–356. doi:10.1016/j.actbio.2019.02.046.

[78] E. Sano, C. Mori, Y. Nashimoto et al., Engineering of vascularized 3D cell constructs to model cellular interactions through a vascular network, Biomicrofluidics 12 (4) (2018) 042204. doi:10.1063/1.5027183.

[79] B. Sacchetti, A. Funari, S. Michienzi et al., Self-Renewing Osteoprogenitors in Bone Marrow Sinusoids Can Organize a Hematopoietic Microenvironment, Cell 131 (2) (2007) 324–336. doi:10.1016/j.cell.2007.08.025.

[80] N. Jusoh, S. Oh, S. Kim et al., Microfluidic vascularized bone tissue model with hydroxyapatite-incorporated extracellular matrix, Lab on a Chip 15 (20) (2015) 3984–3988. doi:10.1039/C5LC00698H.

[81] J. Ahn, J. Lim, N. Jusoh et al., 3D Microfluidic Bone Tumor Microenvironment Comprised of Hydroxyapatite/Fibrin Composite, Frontiers in Bioengineering and Biotechnology 7. doi:10.3389/fbioe.2019.00168.

[82] E. Kunisch, F. Gunnella, S. Wagner et al., The poly (l-lactid-co-glycolide; PLGA) fiber component of brushite-forming calcium phosphate cement induces the osteogenic differentiation of human adipose tissue-derived stem cells, Biomedical Materials 14 (5) (2019) 055012. doi:10.1088/1748-605X/ab3544.

[83] M. B. Sharma, L. S. Limaye V. P. Kale, Mimicking the functional hematopoietic stem cell niche in vitro: recapitulation of marrow physiology by hydrogel-based three-dimensional cultures of mesenchymal stromal cells, Haematologica 97 (5) (2012) 651–660. doi:10.3324/haematol.2011.050500.

[84] S. Sieber, L. Wirth, N. Cavak et al., Bone marrow□on□a□chip: Long□term culture of human haematopoietic stem cells in a three□dimensional microfluidic environment, Journal of Tissue Engineering and Regenerative Medicine 12 (2) (2018) 479–489. doi:10.1002/term.2507.

[85] D. Bexell, S. Gunnarsson, A. Tormin et al., Bone Marrow Multipotent Mesenchymal Stroma Cells Act as Pericyte-like Migratory Vehicles in Experimental Gliomas, Molecular Therapy 17 (1) (2009) 183–190. doi:10.1038/mt.2008.229.

[86] M. Sila-Asna, A. Bunyaratvej, S. Maeda et al., Osteoblast differentiation and bone formation gene expression in strontium-inducing bone marrow mesenchymal stem cell., The Kobe journal of medical sciences 53 (1-2) (2007) 25–35.

[87] Y. Huang, Y. Zhang, X. Ding et al., Osmolarity influences chondrocyte repair after injury in human articular cartilage, Journal of Orthopaedic Surgery and Research 10 (1) (2015) 19. doi:10.1186/s13018-015-0158-z.

[88] A. Labedz-Maslowska, N. Bryniarska, A. Kubiak et al., Multilineage Differentiation Potential of Human Dental Pulp Stem Cells—Impact of 3D and Hypoxic Environment on Osteogenesis In Vitro, International Journal of Molecular Sciences 21 (17) (2020) 6172. doi:10.3390/ijms21176172.

[89] J. Park, B. Park, H. Kim et al., Hypoxia decreases Runx2/Cbfa1 expression in human osteoblast-like cells, Molecular and Cellular Endocrinology 192 (1-2) (2002) 197–203. doi:10.1016/S0303-7207(02)00036-9.

A APPENDIX

Table A.1: Forward and reverse primer sequences used for qPCR

Primer	Forward	Reverse	Soucre
Nestin	AGCGTTGGAACAGAGGTTGG	AGGCTGAGGGACATCTTGAGG	[84]
Fibronectin	CAGACCTATCCAAGCTCAAGTGG	TGGGTGGGATACTCACAGGTC	[84]
Osteocalcin	ATGAGAGCCCTCACACTCCTC	CGTAGAAGCGCCGATAGGC	[86]
Osterix	TAATGGGCTCCTTTCACCTG	CACTGGGCAGACAGTCAGAA	[86]
Collagen I	GATGGATTCCAGTTCGAGTATG	GTTTGGGTTGCTTGTCTGTTTG	[86]
Collagen II	CCTGGCAAAGATGGTGAGACAG	CCTGGTTTTCCACCTTCACCTG	[87]
Collagen X	GCAACTAAGGGCCTCAATGG	CTCAGGCATGACTGCTTGAC	[88]
ICAM-1	CCGACTGGACGAGAGGGATT	TCGGCCCGACAGAGGTAGGT	[84]
Osteonectin	AGTAGGGCCTGGATCTTCTT	CTGCTTCTCAGTCAGAAGGT	[86]
RUNX2	CCCCACGACAACCGCACCAT	CACTCCGGCCCACAAATC	[89]
Osteopontin	CACTGATTTTCCCACGGACCT	CCATTCAACTCCTCGCTTTCC	[84]
GAPDH	GTCAGTGGTGGACCTGACCT	AGGGGAGATTCAGTGTGGTG	[86]

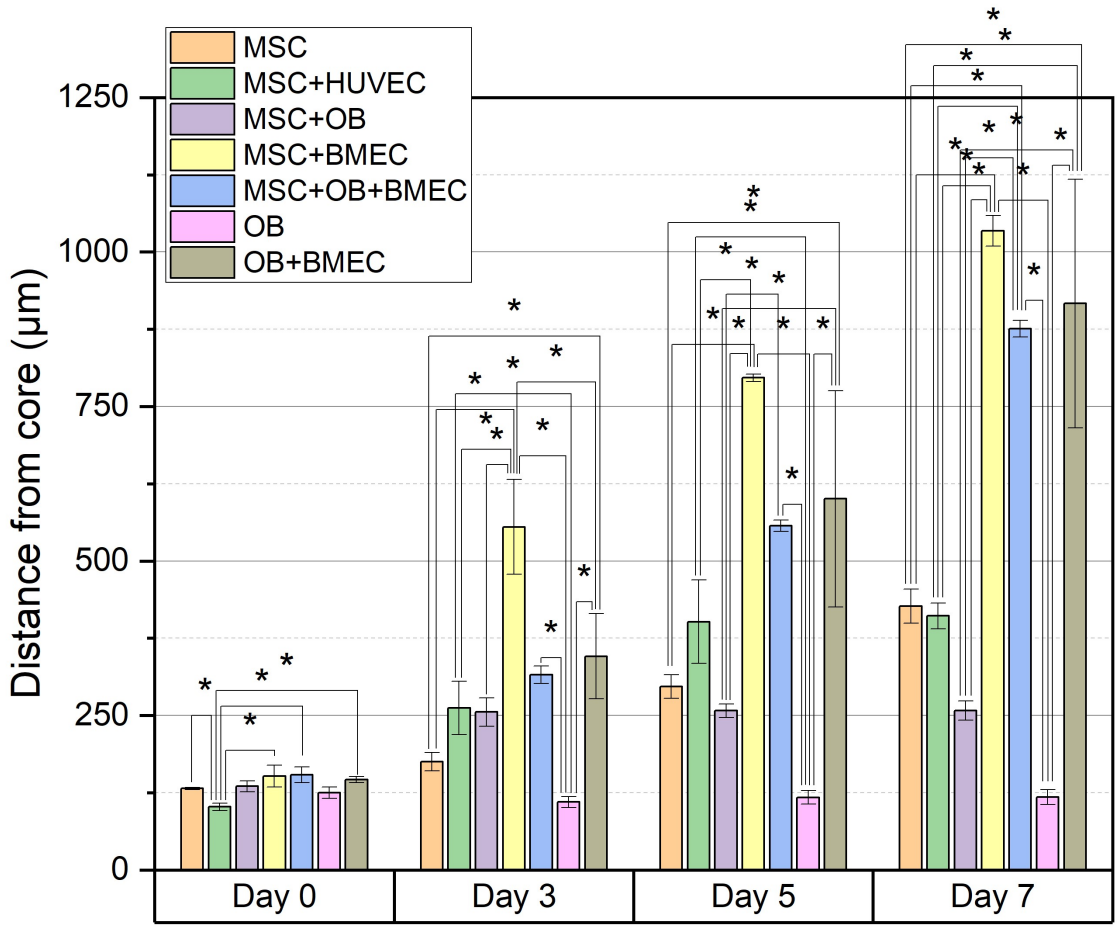

Figure A.1: The distance from the core of the spheroid towards the four furthest sprouts on three different spheroids for every condition on day 0, 3, 5 and 7 with statistical analysis. (*p<0.05)

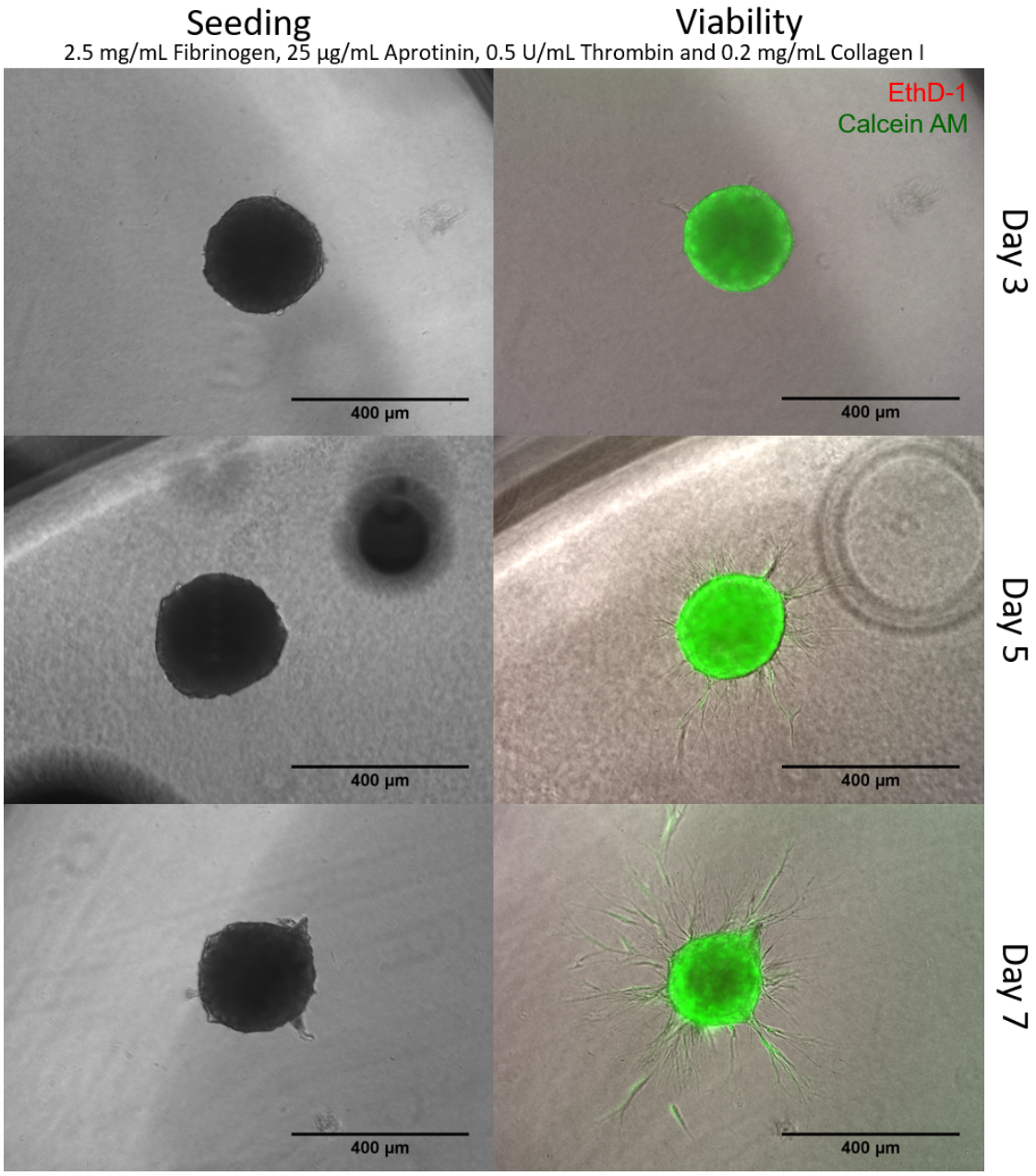

Figure A.2: Spheroids cultured in a Fibrin hydrogel on day 0 and viability staining with Calcein AM and EthD-1 after 3, 5 and 7 days.

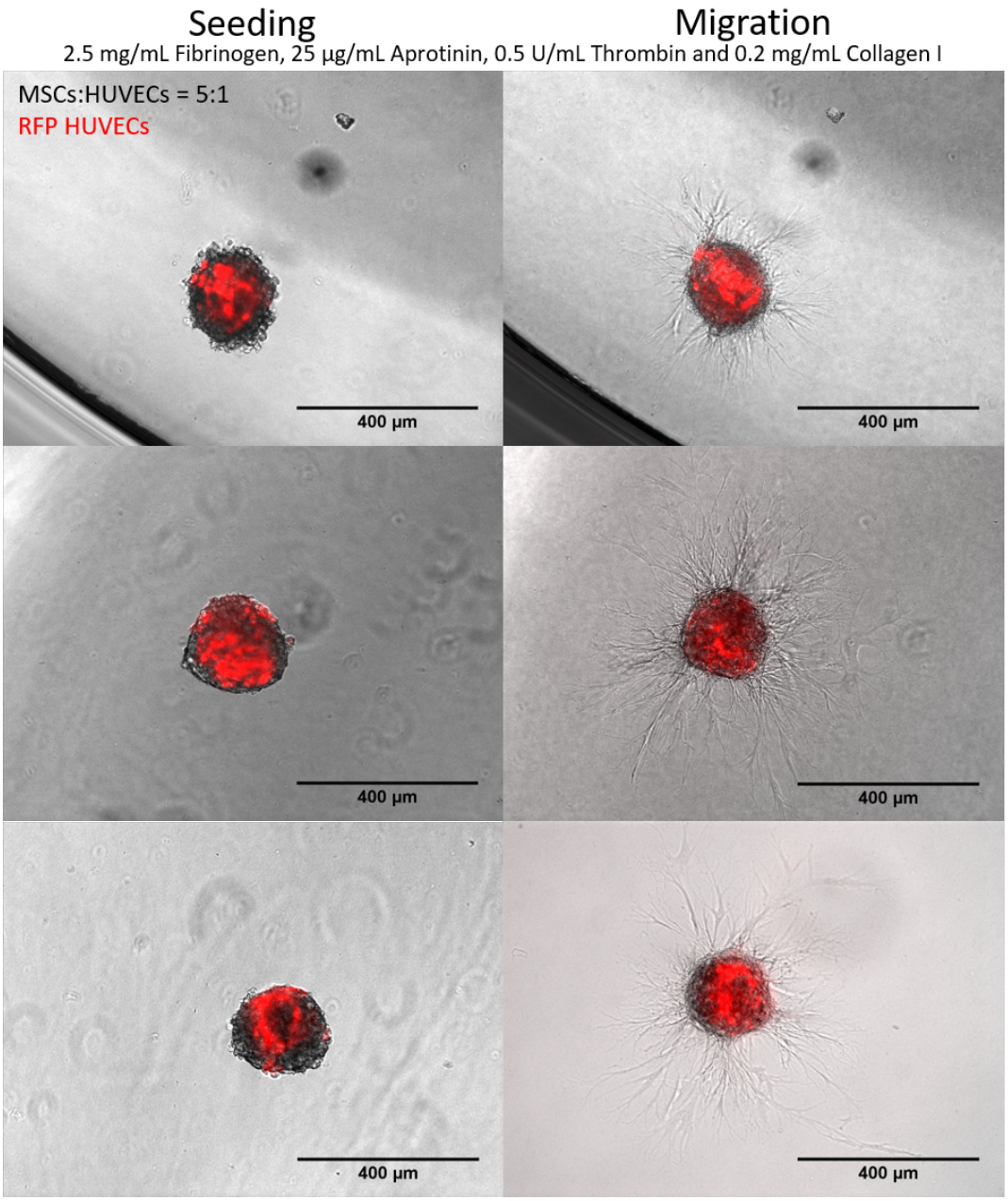

Figure A.3: Co-culture of spheroids with MSCs-RFP HUVECs (5:1) in a Fibrin hydrogel on day 0 and migration after 3, 5 and 7 days.

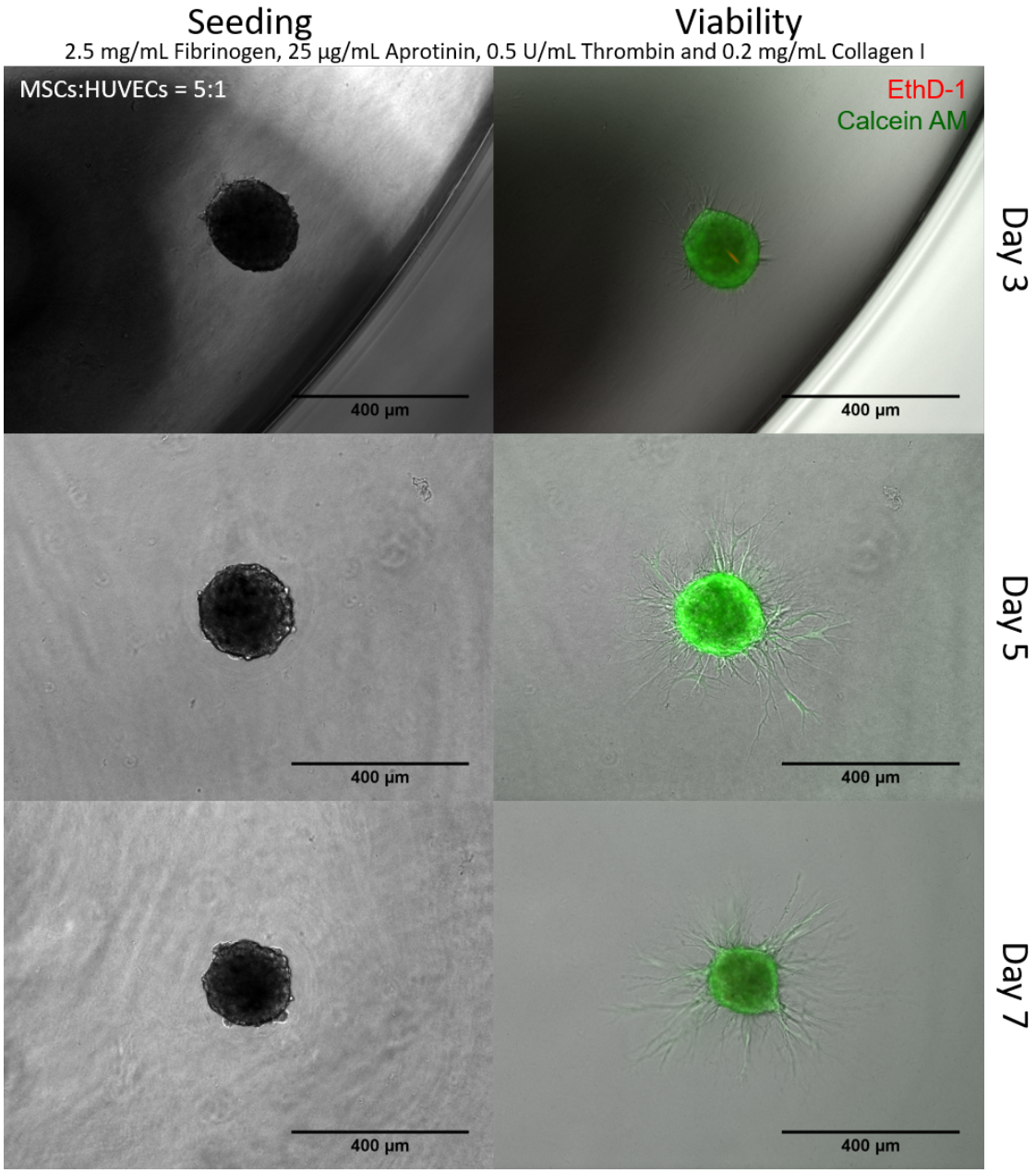

Figure A.4: Co-culture of MSCs-HUVECs (5:1) spheroids in a Fibrin hydrogel, on day 0 and viability staining with Calcein AM and EthD-1 after 3, 5 and 7 days.